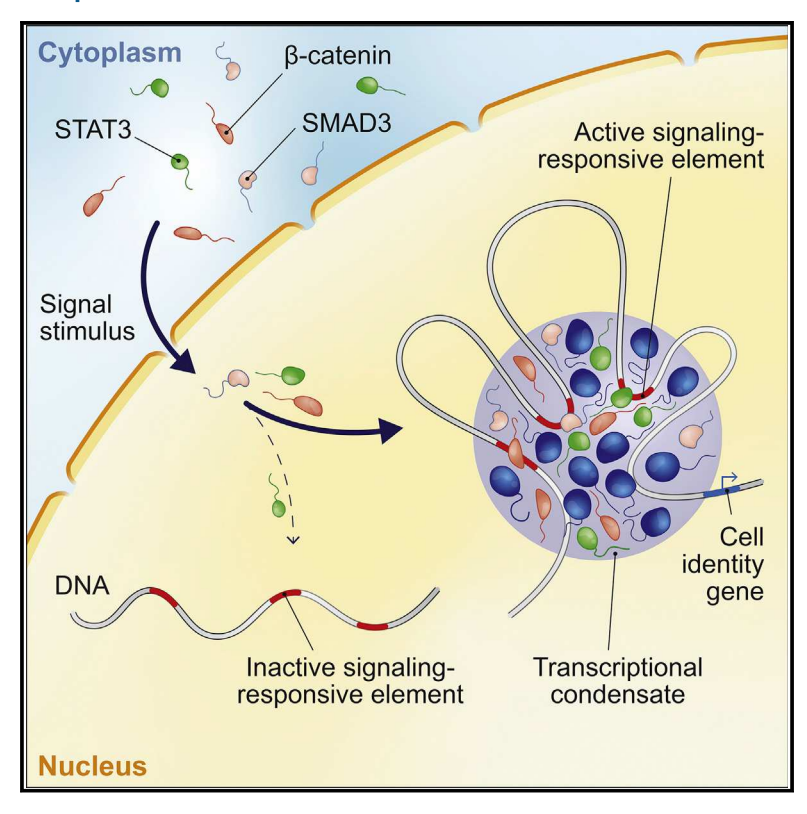
Molecular Cell

Mediator Condensates Localize Signaling Factors to Key Cell Identity Genes

Graphical Abstract



Authors

Alicia V. Zamudio, Alessandra Dall'Agnese, Jonathan E. Henninger, ..., Dylan J. Taatjes, Jurian Schuijers, Richard A. Young

Correspondence

j.schuijers@umcutrecht.nl (J.S.), young@wi.mit.edu (R.A.Y.)

In Brief

Zamudio et al. demonstrate that components of the WNT, TGF- β , and JAK/STAT signaling pathways use their intrinsically disordered regions to condense with Mediator and to target specific genes. These findings provide a model for how context-dependent transcriptional responses can be achieved in cell signaling.

Highlights

- Signaling factors incorporate into Mediator condensates at super-enhancers
- β-Catenin IDRs are required for both phase separation and target gene activation
- Both condensate interactions and TF interactions contribute to β-catenin localization







Mediator Condensates Localize Signaling Factors to Key Cell Identity Genes

Alicia V. Zamudio,^{1,2} Alessandra Dall'Agnese,¹ Jonathan E. Henninger,¹ John C. Manteiga,^{1,2} Lena K. Afeyan,^{1,2} Nancy M. Hannett,¹ Eliot L. Coffey,^{1,2} Charles H. Li,^{1,2} Ozgur Oksuz,¹ Benjamin R. Sabari,¹ Ann Boija,¹ Isaac A. Klein,^{1,3} Susana W. Hawken,⁴ Jan-Hendrik Spille,⁵ Tim-Michael Decker,⁶ Ibrahim I. Cisse,⁵ Brian J. Abraham,^{1,7} Tong I. Lee,¹ Dylan J. Taatjes,⁶ Jurian Schuijers,^{1,8,9,*} and Richard A. Young^{1,2,8,10,*}

SUMMARY

The gene expression programs that define the identity of each cell are controlled by master transcription factors (TFs) that bind cell-type-specific enhancers, as well as signaling factors, which bring extracellular stimuli to these enhancers. Recent studies have revealed that master TFs form phase-separated condensates with the Mediator coactivator at super-enhancers. Here, we present evidence that signaling factors for the WNT, TGF-β, and JAK/ STAT pathways use their intrinsically disordered regions (IDRs) to enter and concentrate in Mediator condensates at super-enhancers. We show that the WNT coactivator β-catenin interacts both with components of condensates and DNA-binding factors to selectively occupy super-enhancer-associated genes. We propose that the cell-type specificity of the response to signaling is mediated in part by the IDRs of the signaling factors, which cause these factors to partition into condensates established by the master TFs and Mediator at genes with prominent roles in cell identity.

INTRODUCTION

Pioneering genetic studies in *Drosophila* showed that transcription factors (TFs) and signaling factors play fundamentally important roles in the control of development (Nüsslein-Volhard and Wieschaus, 1980; Small et al., 1992; van de Wetering et al., 1997; Yan et al., 1996). These and many subsequent studies have led to the understanding that the gene expression programs defining the identity of each cell are controlled by lineage

and cell-typespecific master TFs, which establish cell-type-specific enhancers, and signaling factors, which carry extracellular information to these enhancers (David and Massagué, 2018; Lee and Young, 2013; Mullen and Wrana, 2017; Nusse and Clevers, 2017; Rawlings et al., 2004). Hundreds of different master TFs contribute to the diverse cell-type-specific gene expression programs in an animal, yet a small set of common signaling factors are used to produce cell-type-specific responses to extracellular stimuli. How this is accomplished is not fully understood.

The results of transdifferentiation and reprogramming experiments argue that a small number of master TFs dominate the control of cell-type-specific gene expression (Takahashi and Yamanaka, 2016; Theunissen and Jaenisch, 2014). Although many hundreds of TFs are expressed in each cell type, only a handful are necessary to cause cells to acquire a new identity, as demonstrated by the ability of the TF MyoD to transdifferentiate cells into muscle-like cells (Weintraub et al., 1989) and the ability of the TFs Oct4, Sox2, Klf4, and Myc to reprogram fibroblasts into induced pluripotent stem cells (Takahashi and Yamanaka, 2006). These master TFs dominate the control of gene expression programs by establishing enhancers, and often clusters of enhancers called super-enhancers, at genes with prominent roles in cell identity (Hnisz et al., 2013; Lee and Young, 2013; Whyte et al., 2013).

Cells depend on signaling pathways to maintain their identity and to respond to the extracellular environment. The signaling pathways that play prominent roles in the control of mammalian developmental processes include the WNT, transforming growth factor β (TGF- β), and Janus kinase/signal transducer and activator of transcription (JAK/STAT) pathways (David and Massagué, 2018; Nusse and Clevers, 2017; Rawlings et al., 2004). The terminal signaling factors of the WNT, JAK/STAT, and TGF- β pathways are β -catenin, STAT3, and SMAD3, respectively. In each of these pathways, an extracellular ligand is recognized by a specific receptor, which transduces the signal through



¹Whitehead Institute for Biomedical Research, Cambridge, MA 02142, USA

²Department of Biology, Massachusetts Institute of Technology, Cambridge, MA 02139, USA

³Department of Medical Oncology, Dana-Farber Cancer Institute, Harvard Medical School, Boston, MA 02215, USA

⁴Program in Computational and Systems Biology, Massachusetts Institute of Technology, Cambridge, MA 02139, USA

⁵Department of Physics, Massachusetts Institute of Technology, Cambridge, MA 02139, USA

⁶Department of Biochemistry, University of Colorado, Boulder, Boulder, CO 80303, USA

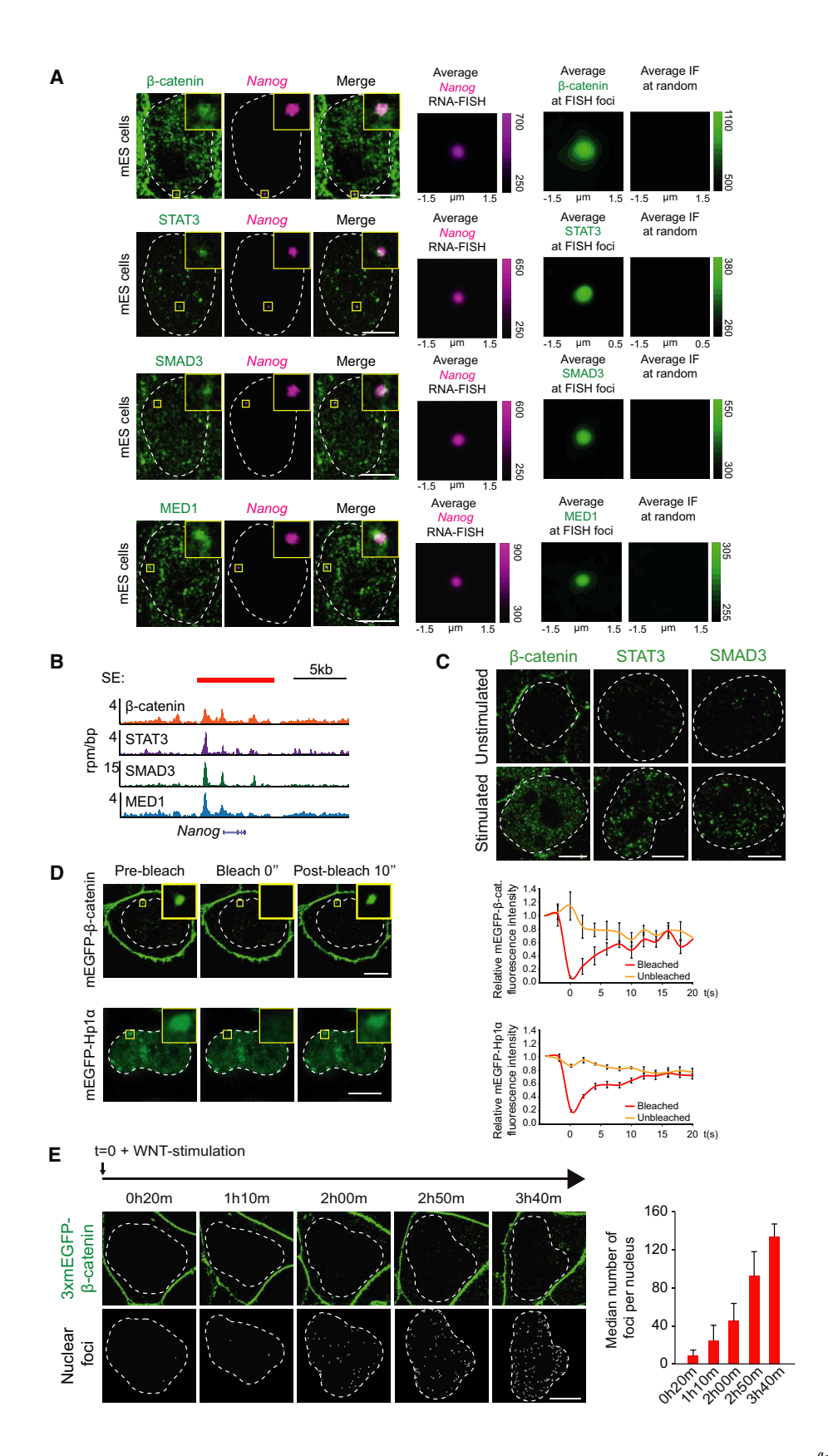
⁷St. Jude Children's Research Hospital, Memphis, TN 38105, USA

⁸These authors contributed equally

⁹Present address: Center for Molecular Medicine, University Medical Center Utrecht, Utrecht 3584CX, the Netherlands

¹⁰Lead Contact

^{*}Correspondence: j.schuijers@umcutrecht.nl (J.S.), young@wi.mit.edu (R.A.Y.) https://doi.org/10.1016/j.molcel.2019.08.016



other proteins to a set of signaling factors that enter the nucleus and occupy signal response elements in the genome. They do this either through interaction with other TFs (the case for β -catenin) or through their own DNA-binding activities (STAT3 and SMAD3) (Darnell et al., 1994; Molenaar et al., 1996; Yingling et al., 1997). In a given cell type, these signaling factors interact with a small subset of a large number of putative signal response elements, preferring to occupy those that occur in the active enhancers of that cell type. This allows for cell-type-specific responses to a common set of signaling factors that are expressed in a broad spectrum of cell types (David and Massagué, 2018; Hnisz et al., 2015; Mullen et al., 2011; Trompouki et al., 2011).

Several mechanisms have been described to account for the ability of signaling factors to preferentially bind the cell-type-specific enhancers and super-enhancers of any one cell type. The WNT signaling factor β-catenin does not have its own DNA-binding domain and is thought to be recruited to genes through interaction with T cell factor/lymphoid enhancer-binding factor (TCF/ LEF) TFs. The SMAD signaling factors can bind with weak affinity to a short DNA motif that is present at high frequency in the mammalian genome, whereas the STAT proteins have relatively long and specific DNA motifs (Farley et al., 2015). The preferred binding by all three signaling factors to active enhancers may reflect, in part, preferred access of these TFs to the "open chromatin" associated with active enhancers (Mullen et al., 2011). These signaling factors may also prefer to bind such sites due to structural changes in the DNA mediated by binding of other TFs at these enhancers (Hallikas et al., 2006; Zhu et al., 2018) or bind cooperatively through direct protein-protein interactions with master TFs (Kelly et al., 2011). These models, however, do not fully explain how a single signaling factor such as β -catenin manages to interact with the cell-type-specific enhancers formed by hundreds of different master TFs.

Recent studies have revealed that master TFs and the Mediator coactivator form phase-separated condensates at superenhancers, which compartmentalize and concentrate the

transcription apparatus at key cell identity genes (Boija et al., 2018; Cho et al., 2018; Sabari et al., 2018). Signaling factors have been shown to have a special preference for cell-type-specific super-enhancers (Hnisz et al., 2015), leading us to postulate that signaling factors may have properties that lead them to partition into transcriptional condensates at super-enhancers, a previously uncharacterized mechanism for cell-type-specific enhancer association. Here, we report that signaling factors are incorporated into condensates with coactivators in response to signaling stimuli at super-enhancer-driven genes in a celltype-specific fashion. β-Catenin is incorporated into Mediator condensates, even when it lacks the domain responsible for interaction with TCF/LEF factors. The optimal occupancy of super-enhancer loci is thus obtained by β-catenin when it contains both condensate-interaction and TF-interaction domains. We propose that phase separation helps achieve the contextdependent specificity of signaling by concentrating signaling factors in master TF-driven transcriptional condensates.

RESULTS

Signal-Dependent Incorporation of Signaling Factors into Condensates at Super-Enhancers

Recent studies have shown that TFs and Mediator form phase-separated condensates at super-enhancers (Boija et al., 2018; Cho et al., 2018; Sabari et al., 2018), and the terminal signaling factors of the WNT, JAK/STAT, and TGF-β pathways (β-catenin, STAT3, and SMAD3, respectively) have been shown to preferentially occupy super-enhancers (Hnisz et al., 2015). To test whether these signaling factors are incorporated into condensates at super-enhancer-associated genes, we performed RNA fluorescence *in situ* hybridization (FISH) for *Nanog* in combination with immunofluorescence (IF) for each of the three signaling factors (Figure 1A). *Nanog*, a gene that is important for pluripotency, is associated with a super-enhancer occupied by these three signaling factors and Mediator in mouse

Figure 1. Signaling Factors Form Signaling-Dependent Condensates at Super-Enhancers In Vivo

(A) Immunofluorescence for β-catenin, STĀT3, SMAD3, and MED1 with concurrent RNĀ-FISH for *Nanog* nascent RNA demonstrating the presence of condensed nuclear foci of the signaling factors at the *Nanog* super-enhancer in mESCs. Cells were grown for 24 h in the presence of CHIR99021, LIF, and activin A to activate the WNT, JAK/STAT, and TGF-β signaling pathways, respectively, before fixation. Hoechst staining was used to determine the nuclear periphery, highlighted with a dotted line. A 100× objective was used for imaging on a spinning disk confocal microscope. Average RNA-FISH signal and average IF signal centered on the RNA-FISH focus for each signaling factor from at least 10 images are shown. Average signaling factor IF signal around randomly selected nuclear positions is displayed in the right-most panel. Scale bars indicate 5 μm.

(B) ChIP-seq tracks displaying occupancy of β-catenin, STAT3, SMAD3, and MED1 in mESCs at the super-enhancer associated with the *Nanog* gene. Read densities are displayed in reads per million per bin (rpm/bin), and the super-enhancer is indicated with a red bar.

(C) Immunofluorescence of mESCs for the signaling factors β -catenin, STAT3, and SMAD3 in unstimulated or stimulated conditions. Cells were stimulated for 24 h with either CHIR99021, LIF, or activin A to activate the WNT, JAK/STAT, and TGF- β signaling pathways, respectively, before fixation. Hoechst staining was used to determine the nuclear periphery, highlighted with a dotted line. A 100× objective was used for imaging on a spinning disk confocal microscope. Scale bars indicate 5 μ m.

(D) Top left: representative images of a FRAP experiment of mEGFP- β -catenin engineered HCT116 cells. The yellow box highlights the punctum undergoing targeted bleaching. Top right: quantification of FRAP data for mEGFP- β -catenin puncta. Bottom left: representative images of a FRAP experiment of mEGFP-HP1 α engineered HCT116 cells. The yellow box highlights the region undergoing targeted bleaching. Bottom right: quantification of FRAP data for mEGFP-HP1 α puncta. The bleaching event occurs at t=0 s. For both the bleached area and the unbleached control, background-subtracted fluorescence intensities are plotted relative to a pre-bleach time point (t=-4 s). Data are plotted as means \pm SEMs (n=9). Images were taken using a Zeiss LSM 880 confocal microscope with Airyscan detector with a 63× objective. Scale bar indicates 2 µm.

(E) Live-cell imaging of endogenously tagged mEGFP-β-catenin in HEK293T cells stimulated with CHIR99021 and imaged over time. Representative images of cells imaged over a 4-h time course are seen in the top panels. Identified foci used for quantification are displayed in the bottom panels. Foci in the nucleus were called and quantified at different time intervals for three biological replicates (right panel). Images were acquired using a Zeiss LSM 880 confocal microscope with Airyscan detector and a 63× objective. Scale bar indicates 2 μm.

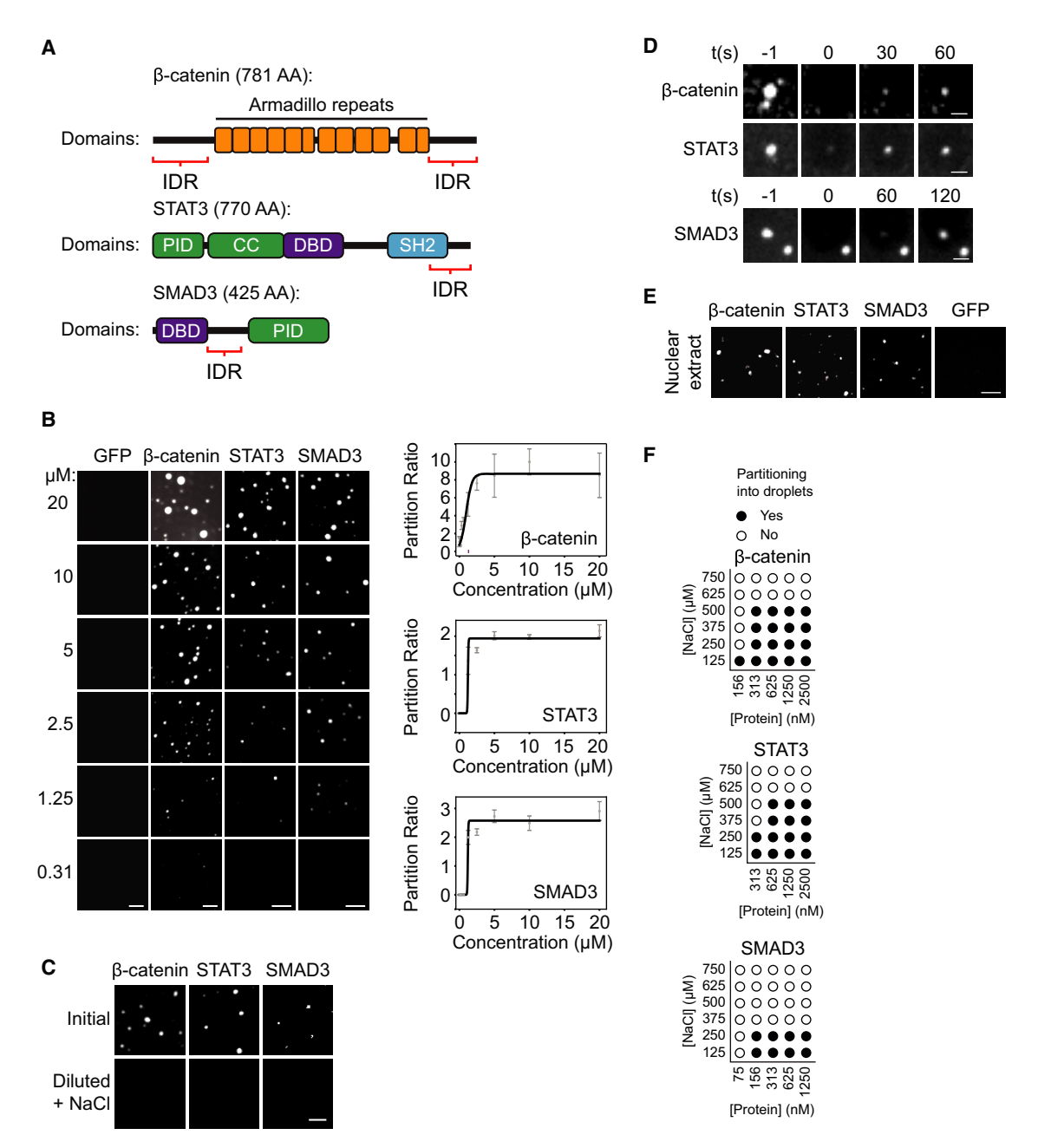


Figure 2. Purified Signaling Factors Can Form Condensates In Vitro

(A) Domain structures of the signaling factors used in this article. CC, coiled-coil domain; DBD, DNA binding domain, DD, dimerization domain; PID, protein interaction domain; SH2: Src homology domain 2. The predicted intrinsically disordered regions (IDRs) are indicated with red brackets.

(B) Representative confocal images of a concentration series of droplet formation assays testing homotypic droplet formation of mEGFP-β-catenin, mEGFP-STAT3, and mEGFP-SMAD3. mEGFP alone is included as a control (left panels). Quantification of the partition ratio for the signaling factors are shown to the right. The partition ratio was calculated by dividing the average fluorescence signal inside the droplets by the average fluorescence signal outside the droplets for at least 10 acquired images at all concentrations tested. All of the assays were performed in the presence of 125 mM NaCl, and 10% PEG-8000 was used as a crowding agent. Scale bars indicate 2 µm.

(C) Dilution droplet assay for the signaling factors. Initial droplets were formed at a protein concentration of 1.25 µM and 125 mM NaCl and imaged. The remaining reaction mixture was then diluted 2-fold, with reaction buffer containing 4 M NaCl to obtain a final salt concentration of 2 M NaCl. Representative images of droplets before and after dilution are displayed.

(D) Representative images of FRAP of in vitro droplets of mEGFP-fused β-catenin, STAT3, and SMAD3 showing recovery after photobleaching in the order of seconds. Droplet formation assays were performed in the presence of 125 mM NaCl and 10% PEG-8000. Scale bars indicate 2 μm. FRAP was performed with a spinning disk confocal miscroscope using a 150× magnification.

(E) Signaling factors form droplets in the presence of nuclear extracts. HEK293T cells were transfected with β-catenin, STAT3, or SMAD3 and nuclear extracts imaged using a spinning disk confocal microscope with a 150× magnification. Scale bar indicates 2 μm.

(legend continued on next page)

embryonic stem cells (mESCs) as shown by chromatin immunoprecipitation sequencing (ChIP-seq) (Figure 1B). We found that condensed foci could be observed for all three factors at the Nanog locus in individual cells (Figure 1A), suggesting that all three factors are incorporated into super-enhancer-associated condensates. Similar results were obtained at an additional super-enhancer locus where transcriptional condensates have been demonstrated to occur in mESCs (Boija et al., 2018; Sabari et al., 2018) (Figures S1A and S1B). To confirm that the association of signaling factors with this locus is cell-type specific, we investigated whether β-catenin condensed foci overlapped with Nanog in C2C12 myoblast cells using a combination of IF and DNA FISH; no β -catenin signal was detected at this locus in C2C12 cells (Figure S1C). These results are consistent with the idea that signaling factors are incorporated into cell-typespecific super-enhancer condensates.

To confirm that the β -catenin, STAT3, and SMAD3 signaling factors are incorporated into nuclear condensates upon pathway stimulation, we performed IF for those factors in mESCs in the presence or absence of the stimulus for each signaling pathway. We found that all three signaling factors were detected as condensed nuclear foci by IF when their respective signaling pathways were activated (Figure 1C). These results indicate that β -catenin, SMAD3, and STAT3 are incorporated into nuclear condensates upon pathway activation.

The condensates formed by TFs and Mediator at super-enhancers exhibit liquid-like behavior (Boija et al., 2018; Cho et al., 2018; Sabari et al., 2018). Hallmarks of liquid-liquid phase-separated condensates are dynamic internal re-organization and rapid exchange kinetics (Banani et al., 2017; Hyman et al., 2014; Shin and Brangwynne, 2017), which can be interrogated by measuring the rate of fluorescence recovery after photobleaching (FRAP). To test whether signaling factors exhibit this type of behavior, we introduced a monomeric EGFP-tag (mEGFP-tag) at the endogenous locus of the β -catenin gene in constitutive WNT-activated HCT116 cells, confirmed that the levels of mEGFP-tagged β-catenin expressed in these cells were similar to those normally expressed in these cells (Figure S1D), and examined the behavior of these puncta by FRAP. The β -catenin nuclear puncta recovered on a timescale of seconds (Figure 1D), with an approximate apparent diffusion coefficient of 0.004 \pm 0.003 μ m²/s. These values are similar to those of previously described components of liquid-like condensates, including euchromatic (Nott et al., 2015; Pak et al., 2016; Sabari et al., 2018) and heterochromatic condensates (Figures 1D and S1D) (Strom et al., 2017; Larson et al., 2017; Zhang et al., 2019), and support the idea that condensates containing β-catenin exhibit liquid-like properties. Together with previous evidence for liquid-like condensates at super-enhancers, which include rapid exchange kinetics and fusion events between condensate components (Cho et al., 2018; Sabari et al., 2018), these results suggest that β-catenin is incorporated and concentrated into these transcriptional condensates.

To investigate the dynamics of β -catenin-containing puncta in response to WNT pathway stimulation, we used HEK293T cells containing an mEGFP tag at the endogenous β -catenin locus, stimulated these cells with a WNT activator, and followed the appearance of nuclear β -catenin puncta in live cells over time. We observed a steady increase in β -catenin-containing nuclear foci for approximately 4 h following stimulation (Figure 1E). These results indicate that β -catenin becomes a component of nuclear condensates in live cells in a WNT-inducible manner.

Purified Signaling Factors Can Form Condensates In Vitro

An analysis of the amino acid sequences of β-catenin, STAT3, and SMAD3 revealed that they contain intrinsically disordered regions (IDRs) (Figures 2A and S2). Because IDRs are capable of forming dynamic networks of weak interactions and have been implicated in condensate formation (Burke et al., 2015; Lin et al., 2015; Nott et al., 2015), we investigated whether these signaling proteins could form phase-separated droplets in vitro. Purified recombinant mEGFP-β-catenin, mEGFP-STAT3, and mEGFP-SMAD3 formed concentration-dependent droplets (Figure 2B). The droplets were spherical, micron sized, and moved freely in solution. The droplet-forming behavior of these proteins exhibited a switch in partition ratio between the dense and dilute phases at micromolar concentrations, which is consistent with the behavior of proteins that undergo phase separation (Figure 2B). Further characterization of these droplets revealed that they were reversible by dilution and sensitive to salt concentration (Figure 2C). The droplets exhibited rapid recovery kinetics after photobleaching (Figure 2D). To determine whether the signaling proteins were able to form droplets in the absence of crowding agents, we expressed mEGFP-tagged forms of the signaling factors in HEK293T cells, created nuclear extracts from these cells, and imaged these extracts. Using this assay we found that all three signaling factors formed droplets in the absence of crowding agents (Figure 2E). We also generated a phase diagram for each of the signaling factors by varying the salt and protein concentrations in the assay, showing that either one phase (dilute) or two phases (dilute and condensed) could be observed at different regimes of the diagram (Figure 2F). These data are consistent with the model that these signaling factors are capable of undergoing liquid-liquid phase separation in vitro.

Purified Signaling Factors Are Incorporated into Mediator Condensates *In Vitro*

The transcriptional condensates formed at super-enhancers contain high concentrations of the Mediator coactivator, and TFs interact with Mediator through the same residues that are important for phase separation of their activation domains (Sabari et al., 2018; Boija et al., 2018). Given the droplet-forming properties of β -catenin, SMAD3, and STAT3 and their localization *in vivo*, we reasoned that these signaling proteins may also interact with and be concentrated into Mediator condensates.

⁽F) Phase diagrams for β-catenin, STAT3, or SMAD3 showing concentrations of salt and protein in which factors separate into a light phase and a dense phase (black dots) and conditions in which only a light phase is present (white dots). Droplet formation assays were performed in the presence of 5% PEG-8000 at the concentrations depicted in the diagram. Droplets were imaged with a spinning disk confocal microscope with a 150× magnification. The partition ratio was calculated for 10 images and proteins were assessed to be in a one- or two-phase regime by comparing the partition ratio to that of an mEGFP control.

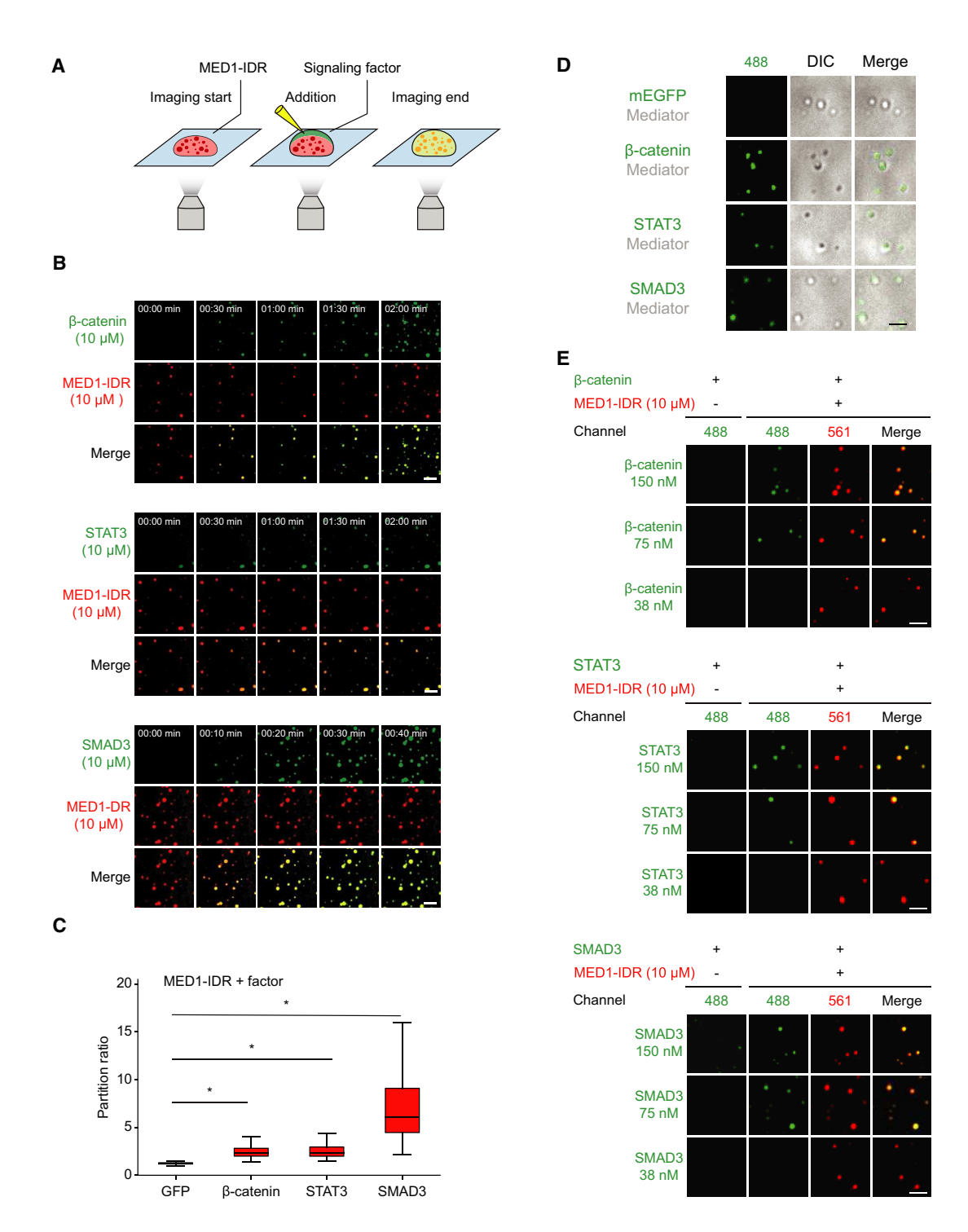


Figure 3. Purified Signaling Factors Are Incorporated into Mediator Condensates In Vitro

(A) Schematic representation of the addition of signaling factor to pre-existing MED1-IDR droplets. mCherry-MED1-IDR droplets were formed and placed in a glass dish and imaged before and after the addition of mEGFP-tagged signaling factors.

(B) Representative images of signaling factor incorporation into MED1-IDR droplets. Preformed mCherry-MED1-IDR droplets were imaged pre- and postaddition of an mEGFP-tagged signaling factor solution for a total of 10 min. Signaling factor was added 30 s after imaging acquisition started. Last image displayed corresponds to the imaging endpoint. A total of 10 μ M MED1-IDR-mCherry in the presence of PEG-8000 was used for droplet formation, and 10 μ M of either mEGFP-β-catenin, mEGFP-SMAD3, or mEGFP-STAT3 in the absence of PEG-8000 was added. Scale bars indicate 2 μm.

(legend continued on next page)

To test this idea, we used MED1-IDR, a surrogate for the Mediator complex (Boija et al., 2018), to form droplets in PEG-8000, added dilute signaling factors to the solution, and monitored the incorporation of signaling factors into MED1-IDR droplets (Figure 3A). We found that β -catenin, SMAD3, and STAT3 were incorporated and concentrated in MED1-IDR droplets (Figures 3B and 3C; Videos S1, S2, and S3). To verify that the signaling factors are also capable of interacting with the full Mediator complex in these droplet assays, droplets were formed with the three signaling factors in combination with purified Mediator complex (Meyer et al., 2008). All three signaling factors, but not mEGFP alone, were able to concentrate into Mediator complex droplets (Figure 3D).

β-Catenin, SMAD3, and STAT3 are found at nanomolar concentrations in mammalian cells (Beck et al., 2011), but the concentrations at which the recombinant signaling proteins form droplets *in vitro* are in the micromolar range (Figure 2B). This led us to investigate whether signaling factors can form droplets at nanomolar concentrations in the presence of MED1-IDR, where they do not form detectable droplets of their own. In these assays, the signaling factors were efficiently partitioned into MED1-IDR droplets (Figure 3E), even when the levels of MED1-IDR were reduced to nanomolar concentrations (Figure S3A). These results are consistent with the possibility that the partitioning of signaling factors into Mediator condensates contributes to the localization of signaling factors to transcriptional condensates at super-enhancers.

Phase Separation of β -Catenin and Activation of Target Genes Are Dependent on IDRs

If the enrichment of signaling factors at super-enhancers occurs through the phase separation properties of their IDRs and incorporation into Mediator condensates, then mutations in the IDRs that affect their ability to form phase-separated droplets in vitro would be expected to affect their ability to target and activate genes in vivo. To test this hypothesis, we focused further studies on β -catenin and sought to identify portions of the protein responsible for its phase separation properties. β-Catenin consists of a central, structured domain with armadillo repeats surrounded by an N-terminal IDR and a C-terminal IDR (Figure 4A). Droplet assays showed that recombinant proteins containing only the armadillo repeats or the N-terminal or C-terminal IDRs were not capable of phase separating at any of the concentrations tested (Figure 4A), suggesting that a combination of multiple domains may be required for condensate formation. To test whether the combination of N-terminal and C-terminal IDRs are sufficient to form phase-separated droplets, a chimeric β-catenin protein was generated in which the central armadillo repeats were replaced by a copy of mEGFP (Figure 4A). When tested in a droplet assay, the chimera protein with both N- and C-terminal IDRs was able to form droplets, albeit slightly smaller and with a lower partition coefficient than the full-length β -catenin (Figures 4A and S4A). If the β -catenin IDRs contribute to phase separation, then condensate formation may be enhanced by doubling their size, which should increase the valence of interactions (Alberti et al., 2019). To test this possibility, we engineered and purified a mutant β -catenin protein containing an extra copy of each IDR. This 2× IDR protein readily formed droplets that were substantially larger than those formed by full-length β -catenin (Figures 4A and S4A). These data suggest that the IDRs of β -catenin are necessary and sufficient for the formation of phase-separated condensates *in vitro*.

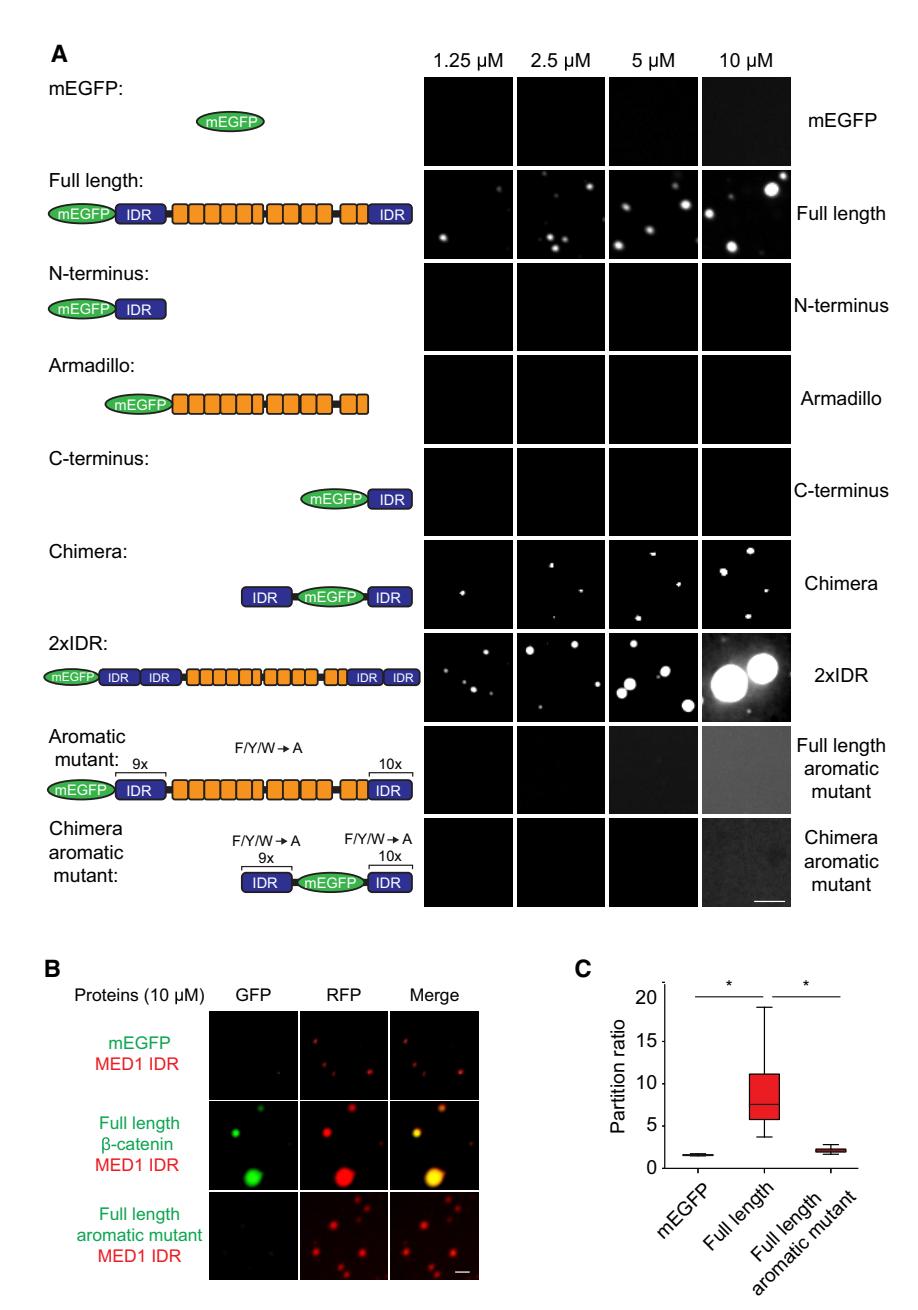
We next focused attention on the amino acid residues within the two IDRs that may contribute to condensation and noted an abundance of aromatic residues (Figure S2). We generated a mutant form of β -catenin and of the chimera protein in which the aromatic residues in both IDRs were substituted with alanines (Figure 4A). These types of mutations perturb pi-cation interactions, which play an important role in the phase separation capacity of multiple proteins (Frey et al., 2018; Wang et al., 2018). When tested in a droplet formation assay, neither the mutant form of β-catenin nor the mutant chimera protein was able to form droplets (Figures 4A and S4A). When tested in a heterotypic droplet formation assay with MED1-IDR, the mutant β -catenin protein failed to incorporate and concentrate into MED1-IDR droplets (Figures 4B and 4C). The mutant form of β -catenin also failed to incorporate into full Mediator droplets (Figure S4B). These results suggest that the aromatic residues in the IDRs of β-catenin contribute to its phase separation behavior.

To test whether the IDRs contribute to the function of β -catenin in vivo, constructs encoding TdTomato-tagged wild-type and aromatic mutant forms of β -catenin under the control of a doxycycline-inducible promoter were integrated into the genome of mESCs (Figures 5A, S5A, and S5C), and ChIP-qPCR for tagged-β-catenin was performed after activation by doxycycline. Wild-type β-catenin was found to occupy the WNTresponsive super-enhancer-associated genes Sp5, Klf4, and Myc, as expected, while lower levels of the aromatic mutant were found at these enhancers using this exogenous expression system (Figure 5B). Expression of these genes was also lower in conditions in which mutant β-catenin was expressed compared to those in which wild-type β -catenin was expressed (Figure 5C). Neither wild-type nor mutant β-catenin factors were found to occupy the typical enhancers of Actrt2 and Fam168b (Figure S5B). Imaging of these exogenous proteins in live cells revealed that the ability of the mutant form of β-catenin to condense was reduced compared to the wild-type form (Figure S5C). These results suggest that the IDRs of β -catenin are

⁽C) Partition ratio was calculated for preformed MED1-IDR-mCherry droplets that were mixed with dilute GFP-tagged signaling factor using the same conditions as in (B). At least 10 images were used for quantification. Droplets were called on merged channels and signal intensity for the GFP-tagged factor in the area within the droplet compared to the intensity of the area outside the droplet. Star indicates p value obtained by a t test <0.05.

⁽D) Representative images of *in vitro* droplet assays of signaling factors, with purified Mediator showing the ability of β -catenin, STAT3, and SMAD3 to interact and partition into intact Mediator droplets. Reactions were performed in the presence of 10% PEG-8000 and 300 nM signaling factor and imaged using a spinning disk confocal microscope with a 150× magnification. Scale bars indicate 2 μ m.

⁽E) Limited dilution droplet assay with near-physiological concentrations of β-catenin, STAT3, and SMAD3. Indicated concentrations of the signaling factors were either added to droplet formation buffer alone (125 mM NaCl and 10% PEG-8000) or in combination with 10 μM MED1-IDR. Scale bars indicate 2 μm.



necessary for both condensate formation and for the proper association and function of β-catenin at super-enhancers in cells that express exogenous β -catenin.

We independently tested the ability of the β-catenin aromatic mutant to transactivate a WNT-responsive reporter gene in a luciferase assay (Figure 5D). Exogenous expression of wildtype β-catenin stimulated luciferase activity, whereas exogenous expression of the aromatic mutant stimulated significantly less activity (Figure 5D). Neither of these forms of β-catenin induced the expression of a WNT-insensitive reporter (Figure S5D). These results are consistent with a model in which β-catenin amino acids that are necessary for condensate formation with Mediator in vitro are also important for gene activation in vivo.

Figure 4. Phase Separation of β-Catenin Is Dependent on Its IDRs

(A) Left: diagram of the different forms of mEGEPβ-catenin proteins tested. Right: representative confocal images of a concentration series of droplet formation assays testing homotypic droplet formation for mEGFP, mEGFP-β-catenin, mEGFP-N-terminal-IDR, mEGFP-armadillo, mEGFP-C-terminal-IDR, mEGFP-chimera, mEGFP-2×IDR, mEGFP-full-length aromatic mutant, and mEGFPchimera-aromatic mutant. Droplet assays were performed in 125 mM NaCl and 10% PEG-8000. Scale bar indicates 1 um.

- (B) Representative confocal images of heterotypic droplet formation assays mixing 10 μM MED1-IDRmCherry with 10 μM of wild-type full-length mEGFP-β-catenin or full-length aromatic mutant mEGFP- β -catenin. Scale bar indicates 1 μ m.
- (C) Partition ratio of factors was quantified for at least 10 images each. Droplets were called on merged channels and signal intensity for the factor in the area within the droplet compared to the intensity of the area outside the droplet. * indicates a p value of < 0.05 in a t test.

β-Catenin-Condensate Interaction Can Occur Independently of TCF/ LEF Factors

β-Catenin does not have DNA-binding activity, and the conventional model for β-catenin recruitment to genes involves a structured interaction between its armadillo repeats and a TCF/LEF family DNAbinding TF. If β-catenin can be recruited to Mediator condensates through dynamic interactions that allow β -catenin to be incorporated into condensates in vivo. then this should occur in the absence of TCF/LEF factors. We developed a series of assays to test this idea.

We investigated whether β -catenin could be incorporated into MED1 condensates in vivo by using a previously developed lac-array assay (Janicki et al., 2004) (Figure 6A). The MED1-IDR was tethered to an array of LacI-binding sites in U2OS cells,

which have a constitutively activated WNT signaling pathway (Chen et al., 2015) and thus have detectable levels of β -catenin in the nucleus. Cells were transiently transfected with either LacI-MED1-IDR or control LacI. The LacI-MED1-IDR, but not Lacl alone, was found to recruit endogenous β-catenin to the lac array (Figure 6A). This effect was likely not mediated through interactions with TCF/LEF and direct interaction with DNA because the lac array does not contain TCF motifs and no TCF/ LEF family member was detected at LacI-MED1-IDR foci by IF (Figure S6A). The heterochromatin-binding protein HP1 α served as a control and was also not recruited to the array (Figure S6B). When TdTomato-labeled wild-type and aromatic mutant β-catenin were ectopically expressed, the TdTomato-labeled wild-type

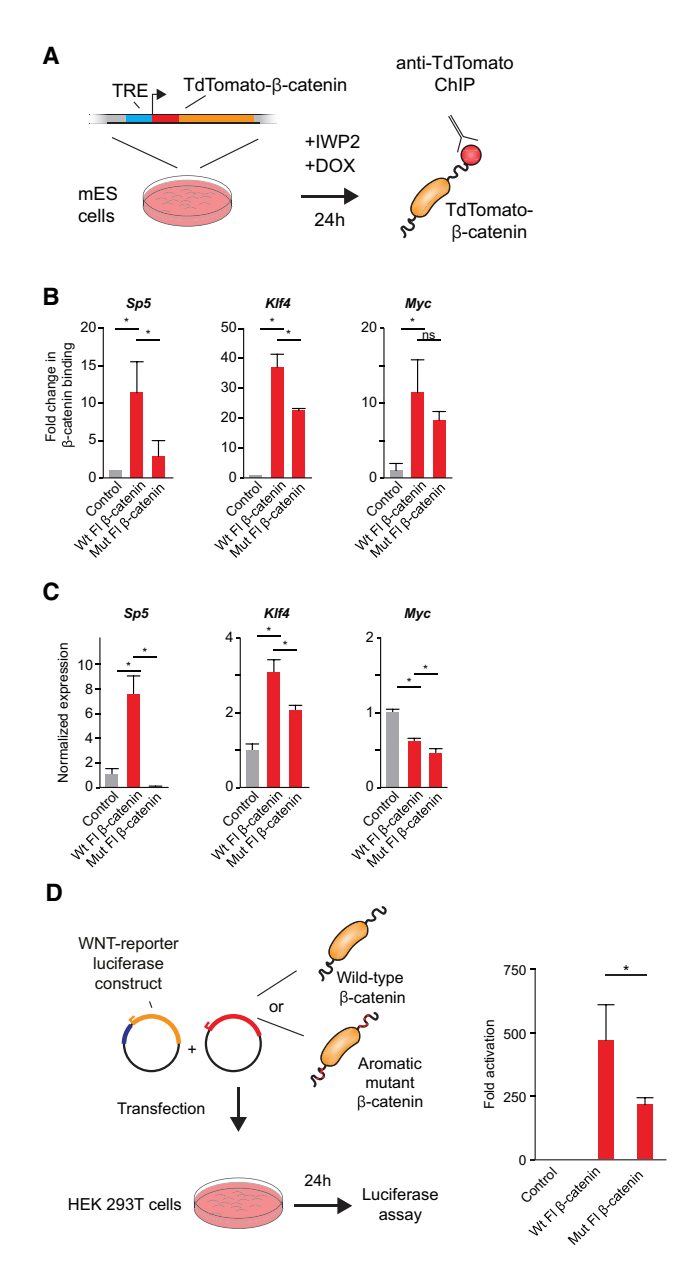


Figure 5. Localization of β -Catenin and Activation of Target Genes Is Dependent on Its IDRs

(A) Schematic of the ChIP experiment. TdTomato-tagged wild-type or aromatic mutant β -catenin were stably integrated in mESCs under a doxycycline-inducible promoter. Doxycycline and an inhibitor of the WNT pathway were added to the media 24 h before crosslinking. ChIP was performed using antibodies against TdTomato. TRE, tetracycline-responsive element.

(B) ChIP-qPCR of ectopically expressed wild-type and aromatic mutant β-catenin at *Myc*, Sp5, and *Klf4* enhancers. Error bars indicate SDs of three replicates. Stars indicate p values obtained by a t test <0.05.

(C) qRT-PCR of mRNA levels after ectopic expression of wild-type or aromatic mutant β -catenin of Myc, Sp5, and $\mathit{Klf4}$. Error bars indicate SDs of three replicates. Stars indicate p values obtained by a t test <0.05.

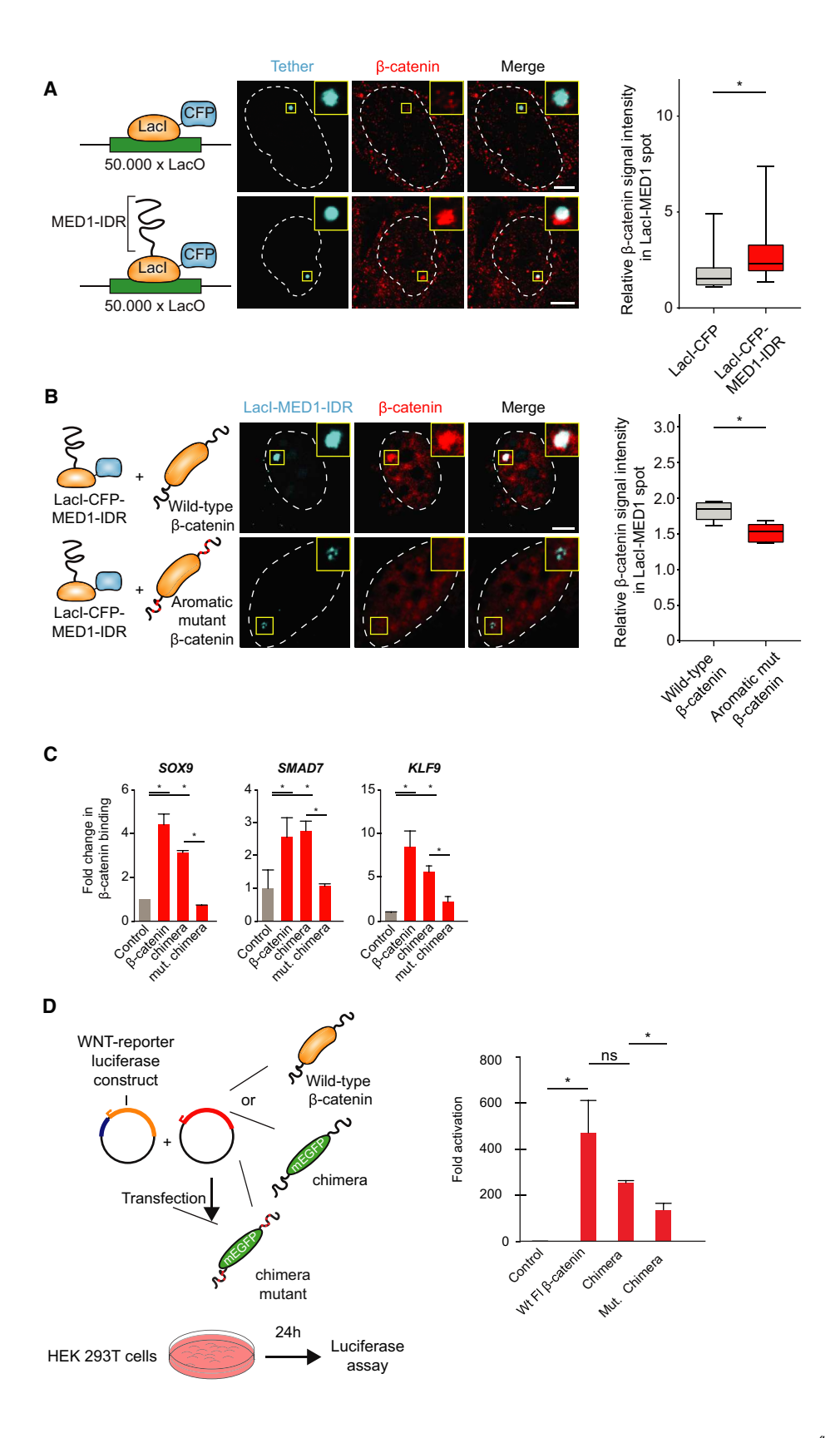
(D) Luciferase assay using a synthetic WNT reporter containing 10 copies of the consensus TCF/LEF motif in which wild-type or aromatic mutant was over-expressed in HEK293T cells. An average of three biological replicates is shown. Error bars show the SD. Star indicates p value obtained by a t test <0.05.

β-catenin accumulated at the MED1-IDR-occupied lac array, while accumulation of the TdTomato-labeled aromatic mutant was significantly reduced (Figure 6B). In addition, when transcription of CFP from the lac-array locus was assayed by qRT-PCR, the wild-type β -catenin induced significantly stronger expression than the mutant β -catenin (Figure S6G). The β -catenin aromatic mutant maintained its ability to interact with TCF/LEF factors based on a co-immunoprecipitation assay with TCF7L2 in HEK293T cells (Figure S6C). These results suggest that β -catenin can be incorporated into MED1-IDR condensates *in vivo* in the absence of TCF/LEF family members and in a manner that is dependent on the same amino acids that are required for β -catenin to be incorporated and concentrated into Mediator condensates *in vitro*.

To further test whether the regions of β-catenin that allow it to be incorporated into a condensate with Mediator are sufficient to address β -catenin to specific genomic loci in the absence of an interaction with TCF/LEF factors, we engineered a HEK293T cell line in which β -catenin, the β -catenin-chimera, or the β -catenin-chimera mutant was integrated under the control of a doxycycline-inducible promoter (Figure S6E). ChIP-qPCR for GFP showed enrichment for wild-type β -catenin and β -cateninchimera but not the aromatic mutant chimera at the WNT-driven super-enhancer genes SOX9, SMAD7, and KLF9 (Figure 6C). Two typical enhancers showed no enrichment for any of the tagged factors, indicating that the IDRs of β-catenin are sufficient to address mEGFP to specific genomic loci (Figure S6D). This effect was not due to differences in the expression of these factors, as the chimera and mutant chimera expressed at levels comparable to the wild-type form of β-catenin (Figure S6E). The C-terminal IDR of β-catenin contains its transactivation domain, so we sought to investigate whether the β-catenin-chimera may also be able to activate transcription and localize to the correct genomic locations. When the β-catenin-chimera was overexpressed in a luciferase reporter assay, it was able to activate a WNT reporter (Figure 6D). None of these forms of β-catenin were able to robustly activate the expression of a WNT unresponsive reporter (Figure S6F). These data are consistent with the idea that β -catenin can be recruited to a Mediator condensate, at least partially, through its ability to interact with this condensate and independently of its classical interaction with TCF/LEF factors.

Both Intrinsically Disordered and Armadillo Domains Enable Selective Occupancy of Super-Enhancer Genes

Our evidence, together with that of prior studies on the structured armadillo domain (Behrens et al., 1996; Molenaar et al., 1996; van de Wetering et al., 1997), suggest that β -catenin interacts with super-enhancers through both the condensate interaction properties of its IDRs and the TF interaction properties of the armadillo repeat domain. A prediction of this model is that full-length β -catenin, the IDR chimera alone, and the armadillo repeats alone may have the ability to be incorporated into super-enhancer loci in cells. To test this prediction, we engineered endogenously tagged mEGFP- β -catenin mESCs and mESCs expressing integrated mEGFP-tagged armadillo repeats (armadillo) or mEGFP-tagged IDRs (chimera) under the control of a doxycycline-inducible promoter (Figures 7A and S7A). The mESCs express the TCF/LEF factor TCF3, which we have previously shown



occupies enhancers with master TFs, and thus provides a DNA-anchoring interaction with β -catenin (Hnisz et al., 2015). An anti-GFP antibody was used to conduct ChIP-seq in all three cell lines, and the results revealed that both the armadillo repeat protein and the chimeric IDR protein are similarly associated with super-enhancers (Figures 7B, 7C, and S7B). The full-length β -catenin protein produced a higher signal than either of the proteins consisting of its components (Figures 7B and 7C), which is consistent with the notion that both IDR and armadillo-repeat components have roles in localizing to super-enhancers. These results are consistent with the model that both the condensate interaction properties of the IDRs of β -catenin and the structured TF interaction properties of its armadillo repeat domain contribute to selective occupancy at super-enhancers.

DISCUSSION

Diverse cell types use a small set of shared, developmentally important signaling pathways to transmit extracellular information to modify gene expression programs (Perrimon et al., 2012). In any one cell type, effector components of the WNT, TGF- β , and JAK/STAT pathways connect to only a small subset of a large number of potential signal response elements, preferring to bind those in active enhancers formed by the master TFs of that cell type, thus producing cell-type-specific responses (David and Massagué, 2018; Hnisz et al., 2015; Mullen et al., 2011; Trompouki et al., 2011). The mechanisms that have been described to account for this bias include preferential access to "open chromatin" (Mullen et al., 2011), to altered DNA structures caused by binding of other TFs, and to cooperative proteinprotein interactions with master TFs (Hallikas et al., 2006; Kelly et al., 2011). The observation that signaling factors have a special preference for cell-type-specific super-enhancers (Hnisz et al., 2015), coupled with the finding that TFs and Mediator form phase-separated condensates at super-enhancers (Boija et al., 2018; Cho et al., 2018; Sabari et al., 2018), led us to investigate whether signaling factors have properties that facilitate partitioning into transcriptional condensates at super-enhancers. The evidence described here argues that the cell-type-dependent specificity of signaling may be achieved, at least in part, by addressing signaling factors to transcriptional condensates at super-enhancers. In this manner, the specificity of the response to signaling can be achieved through the combination of signaling factor incorporation into the condensate compartment and through interaction with DNA or DNA-binding factors.

We find that the signaling factors β -catenin, STAT3, and SMAD3 occur in condensed puncta at signal-responsive super-enhancers in ESCs, where transcriptional condensates have been reported to contain hundreds of molecules of Mediator and RNA polymerase II (Boija et al., 2018; Cho et al., 2018; Sabari et al., 2018). These signaling factors can be incorporated and concentrated into Mediator condensates in vitro, suggesting that their ability to enter Mediator condensates may contribute to their preferential association with Mediator condensates found at super-enhancers in vivo. Tethering a Mediator subunit to an array of genomic sites forms a condensate that can recruit at least one of these signaling factors, β -catenin, to the condensate and does so in the absence of a structured interaction with its classic partner, the DNA-binding factor TCF7L2. In addition, we find that the β -catenin IDRs alone and the TF-binding armadillo repeat alone can be recruited to super-enhancer loci genome-wide; optimal recruitment requires both intrinsically disordered and armadillo domains.

Condensate formation at super-enhancers provides a compartment to concentrate the transcription apparatus at highly expressed genes that play prominent roles in cell identity (Boija et al., 2018; Cho et al., 2018; Sabari et al., 2018). The results described here indicate that these condensates can also compartmentalize signaling factors, which helps explain why signaling factors are preferentially recruited to super-enhancer loci (Hnisz et al., 2015). In the absence of the ability to interact with DNA or a DNA-binding factor, the signaling factors are free to exit the condensate, so we suggest that it is the combination of condensate-mediated concentration of signaling factors and DNA binding that provides the exquisite specificity and high level of gene activation that are characteristic of signaling.

The model we describe for β -catenin entry into superenhancer condensates may help explain additional conundrums in the signaling literature. For example, β -catenin has been reported to interact with a large number of different proteins (Schuijers et al., 2014) and this interaction promiscuity has resulted in the proposal that a large number of DNA-binding TFs have the capacity to recruit β -catenin in addition to the canonical recruiters of the TCF/LEF family (Nateri et al., 2005; Kouzmenko et al., 2004; Essers et al., 2005; Kaidi et al., 2007; Botrugno et al., 2004; Kelly et al., 2011; Sinner et al., 2004). However, the majority of these reported interactions were not supported by functional data, and only binding to TCF has been supported by co-crystallization (Poy et al., 2001; Sampietro et al., 2006). Our model may explain how β -catenin could functionally interact

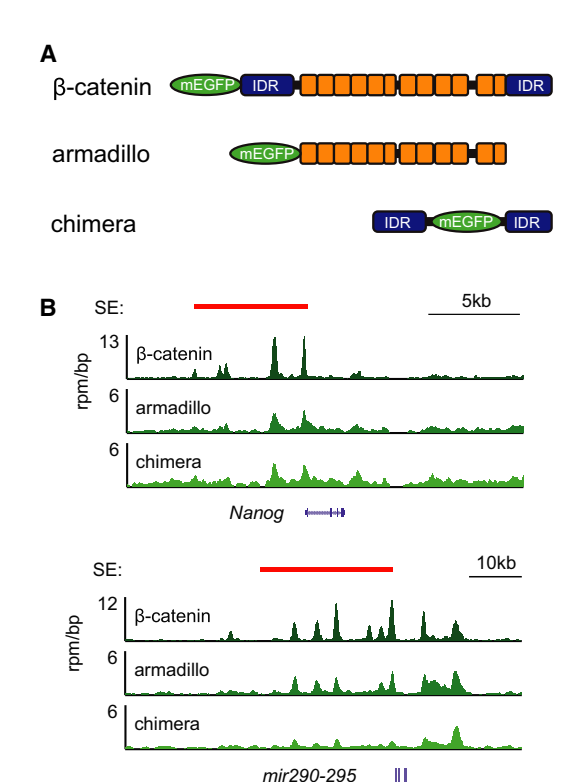
Figure 6. $\beta\text{-}Catenin\text{-}Condensate Interaction Can Occur Independently of TCF/LEF Factors}$

(A) Immunofluorescence of β -catenin in Lac-U2OS cells transfected with an Lac-binding domain-CFP or an Lac-binding domain-CFP-MED1-IDR construct, imaged with a $100 \times$ magnification on a spinning disk confocal microscope. Hoechst staining was used to determine the nuclear periphery, highlighted with a dotted line. Quantification shows the relative intensity of β -catenin in CFP foci. Scale bar indicates 5 μ m. * indicates a p value of < 0.05 in a t test.

(B) Fluorescence imaging of overexpressed TdTomato-tagged wild-type or aromatic mutant β -catenin in U2OS 2-6-3 cells co-transfected with an Lac-binding domain-CFP or an Lac-binding domain-CFP-MED1-IDR construct, imaged with a 100× magnification on a spinning disk confocal microscope. Hoechst staining was used to determine the nuclear periphery, highlighted with a dotted line. Quantification shows the relative intensity of overexpressed β -catenin forms in called CFP foci. Scale bar indicates 5 μ m. *p < 0.05, t test.

(C) ChIP-qPCR for β-catenin-GFP-chimera and chimera mutant at the enhancers of SOX9, SMAD7, and KLF9 in HEK293T cells. Error bars show the SD of the mean. Stars indicate p values obtained by a t test <0.05.

(D) Luciferase assay of cells overexpressing β-catenin-mEGFP-chimera or mutant chimera in combination with a synthetic WNT reporter containing 10 copies of the consensus TCF/LEF motif. Average of three biological replicates is shown. Untransfected control and wild-type (Wt) FL-β-catenin came from the same experiment and are the same as in Figure 5, but displayed in two different graphs. Error bars show the SD. Stars indicate p values obtained by a t test <0.05.



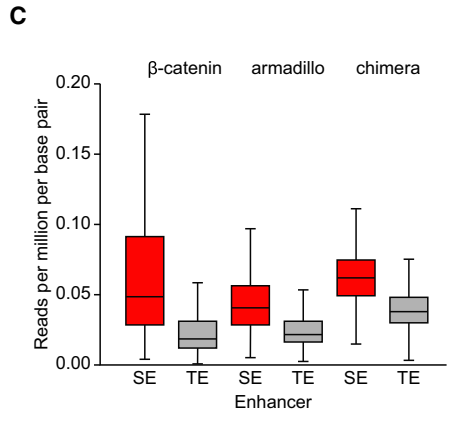


Figure 7. Both IDRs and Armadillo Domains Enable Selective Occupancy of Super-Enhancer Genes

(A) Cartoon depicting the different forms of β -catenin used in ChIP-seq experiments.

(B) ChIP-seq tracks of Nanog and mir290 showing binding of β-cateninarmadillo repeats and IDRs to super-enhancer-associated genes. Read densities are displayed in reads per million per bin (rpm/bin), and the superenhancer is indicated with a red bar.

(C) Quantification of ChIP-seq read densities of super-enhancers (SE) and typical enhancers (TE) of the different forms of β -catenin.

with a large number of TFs in a transcriptional condensate, yet fail to activate transcription in an artificial system in which such a condensate may not be assembled.

The condensate model described here may also apply to additional signaling pathways such as those of the Notch, Hedgehog, and receptor tyrosine kinase pathways. The condensate model may also facilitate further understanding of pathological signaling in diseases such as cancer. Dysregulated transcription and signaling are in fact two hallmarks of cancer (Bradner et al., 2017). Cancer cells develop genomic alterations that create super-enhancers at driver oncogenes (Chapuy et al., 2013; Hnisz et al., 2013; Lin et al., 2016; Mansour et al., 2014; Zhang et al., 2016), and these oncogenes are especially responsive to oncogenic signaling (Hnisz et al., 2015). The signaling factors that contribute to oncogenic signaling may generally interact with super-enhancer condensates through properties that also promote phase separation. In this way, tumor cells dependent on a particular signaling pathway could acquire resistance to therapies by using alternative signaling pathways whose signaling factors could incorporate into transcriptional condensates. Perhaps therapies that target both oncogenic signaling pathways and super-enhancer components will prove especially effective in tumor cells that have signaling and transcriptional dependencies.

STAR*METHODS

Detailed methods are provided in the online version of this paper and include the following:

- KEY RESOURCES TABLE
- LEAD CONTACT AND MATERIALS AVAILABILITY
- EXPERIMENTAL MODEL AND SUBJECT DETAILS
 - Cell lines
 - Cell culture conditions
 - O Cell line stimulation
 - Cell line generation
- **METHOD DETAILS**
 - O FRAP
 - Immunofluorescence
 - O Co-Immunofluorescence with DNA FISH
 - O Co-Immunofluorescence with RNA FISH
 - Protein purification
 - In vitro droplet formation assay
 - Droplet Assays in Nuclear Extract
 - Purification of Mediator
 - O RT-qPCR
 - O ChIP
- QUANTIFICATION AND STATISTICAL ANALYSIS
 - FRAP quantification
 - Average image analysis
 - Heterotypic droplet analysis
- O ChIP-seq analysis
- DATA AND CODE AVAILABILITY

SUPPLEMENTAL INFORMATION

Supplemental Information can be found online at https://doi.org/10.1016/j. molcel.2019.08.016.

ACKNOWLEDGMENTS

We thank the Whitehead Institute Genome Technology Core, FACS facility, Keck Imaging Facility, and Harvard Center for Biological Imaging for their assistance. We thank Krishna Shrinivas for help with the quantification of the FRAP data. This work is supported by NIH grant GM123511 (to R.A.Y.), National Science Foundation (NSF) grant PHY1743900 (to R.A.Y.), funds from Novo Nordisk (to R.A.Y.), NIH grant GM117370 (to D.J.T.), an NSF Graduate Research Fellowship (to A.V.Z.), NIH grant T32CA009172 (to I.A.K.), NIH Director's New Innovator award DP2CA195769 (to I.I.C.), NIH grant GM134734 (to I.I.C.), Pew Charitable Trusts' Pew Biomedical Scholars Program grant (to I.I.C.), Deutsch Forschungsgemeinschaft (DFG) Research Fellowship DE 3069/1-1 (to T.-M.D.), and Swedish Research Council Postdoctoral Fellowship VR 2017-00372 (to A.B.).

AUTHOR CONTRIBUTIONS

Conceptualization, J.S., A.V.Z., and R.A.Y.; Methodology, J.S. and A.V.Z.; Software & Formal Analysis, J.S., A.V.Z., C.H.L., and J.E.H.; Investigation, J.S., A.V.Z., A.D., J.H., J.C.M., N.M.H., L.K.A., E.L.C., A.B., B.R.S., S.W.H., J.-H.S., I.I.C., T.-M.D., and D.J.T.; Writing, J.S., A.V.Z., T.I.L., and R.A.Y.; Visualization, J.S. and A.V.Z.; Supervision, J.S. and R.A.Y.; Funding Acquisition, R.A.Y.

DECLARATION OF INTERESTS

The Whitehead Institute plans to file a patent application based in part on this paper. R.A.Y. is a founder and shareholder of Syros Pharmaceuticals, Camp4 Therapeutics, Omega Therapeutics, and Dewpoint Therapeutics. B.J.A. and T.I.L. are shareholders of Syros Pharmaceuticals. T.I.L. is a consultant to Camp4 Therapeutics.

Received: February 14, 2019 Revised: June 14, 2019 Accepted: August 16, 2019 Published: September 25, 2019

REFERENCES

Alberti, S., Gladfelter, A., and Mittag, T. (2019). Considerations and Challenges in Studying Liquid-Liquid Phase Separation and Biomolecular Condensates. Cell 176, 419–434.

Banani, S.F., Lee, H.O., Hyman, A.A., and Rosen, M.K. (2017). Biomolecular condensates: organizers of cellular biochemistry. Nat. Rev. Mol. Cell Biol. 18, 285–298.

Beck, M., Schmidt, A., Malmstroem, J., Claassen, M., Ori, A., Szymborska, A., Herzog, F., Rinner, O., Ellenberg, J., and Aebersold, R. (2011). The quantitative proteome of a human cell line. Mol. Syst. Biol. 7, 549.

Behrens, J., von Kries, J.P., Kühl, M., Bruhn, L., Wedlich, D., Grosschedl, R., and Birchmeier, W. (1996). Functional interaction of beta-catenin with the transcription factor LEF-1. Nature *382*, 638–642.

Boija, A., Klein, I.A., Sabari, B.R., Dall'Agnese, A., Coffey, E.L., Zamudio, A.V., Li, C.H., Shrinivas, K., Manteiga, J.C., Hannett, N.M., et al. (2018). Transcription Factors Activate Genes through the Phase-Separation Capacity of Their Activation Domains. Cell *175*, 1842–1855.e16.

Botrugno, O.A., Fayard, E., Annicotte, J.-S., Haby, C., Brennan, T., Wendling, O., Tanaka, T., Kodama, T., Thomas, W., Auwerx, J., and Schoonjans, K. (2004). Synergy between LRH-1 and beta-catenin induces G1 cyclin-mediated cell proliferation. Mol. Cell *15*, 499–509.

Bradner, J.E., Hnisz, D., and Young, R.A. (2017). Transcriptional Addiction in Cancer. Cell *168*, 629–643.

Burke, K.A., Janke, A.M., Rhine, C.L., and Fawzi, N.L. (2015). Residue-by-Residue View of In Vitro FUS Granules that Bind the C-Terminal Domain of RNA Polymerase II. Mol. Cell *60*, 231–241.

Chapuy, B., McKeown, M.R., Lin, C.Y., Monti, S., Roemer, M.G.M., Qi, J., Rahl, P.B., Sun, H.H., Yeda, K.T., Doench, J.G., et al. (2013). Discovery and characterization of super-enhancer-associated dependencies in diffuse large B cell lymphoma. Cancer Cell *24*, 777–790.

Chen, C., Zhao, M., Tian, A., Zhang, X., Yao, Z., and Ma, X. (2015). Aberrant activation of Wnt/ β -catenin signaling drives proliferation of bone sarcoma cells. Oncotarget 6, 17570–17583.

Cho, W.K., Spille, J.H., Hecht, M., Lee, C., Li, C., Grube, V., and Cisse, I.I. (2018). Mediator and RNA polymerase II clusters associate in transcription-dependent condensates. Science *361*, 412–415.

Darnell, J., Kerr, I., and Stark, G. (1994). Jak-STAT pathways and transcriptional activation in response. Science 264, 1415–1421.

David, C.J., and Massagué, J. (2018). Contextual determinants of TGFβ action in development, immunity and cancer. Nat. Rev. Mol. Cell Biol. 19, 419–435.

Essers, M.A.G., de Vries-Smits, L.M.M., Barker, N., Polderman, P.E., Burgering, B.M.T., and Korswagen, H.C. (2005). Functional interaction between beta-catenin and FOXO in oxidative stress signaling. Science *308*, 1181–1184.

Farley, E.K., Olson, K.M., Zhang, W., Brandt, A.J., Rokhsar, D.S., and Levine, M.S. (2015). Suboptimization of developmental enhancers. Science *350*, 325–328.

Frey, S., Rees, R., Schünemann, J., Ng, S.C., Fünfgeld, K., Huyton, T., and Görlich, D. (2018). Surface Properties Determining Passage Rates of Proteins through Nuclear Pores. Cell *174*, 202–217.e9.

Hallikas, O., Palin, K., Sinjushina, N., Rautiainen, R., Partanen, J., Ukkonen, E., and Taipale, J. (2006). Genome-wide prediction of mammalian enhancers based on analysis of transcription-factor binding affinity. Cell *124*, 47–59.

Hnisz, D., Abraham, B.J., Lee, T.I., Lau, A., Saint-André, V., Sigova, A.A., Hoke, H.A., and Young, R.A. (2013). Super-enhancers in the control of cell identity and disease. Cell *155*, 934–947.

Hnisz, D., Schuijers, J., Lin, C.Y., Weintraub, A.S., Abraham, B.J., Lee, T.I., Bradner, J.E., and Young, R.A. (2015). Convergence of developmental and oncogenic signaling pathways at transcriptional super-enhancers. Mol. Cell 58, 362–370.

Hyman, A.A., Weber, C.A., and Jülicher, F. (2014). Liquid-liquid phase separation in biology. Annu. Rev. Cell Dev. Biol. *30*, 39–58.

Janicki, S.M., Tsukamoto, T., Salghetti, S.E., Tansey, W.P., Sachidanandam, R., Prasanth, K.V., Ried, T., Shav-Tal, Y., Bertrand, E., Singer, R.H., and Spector, D.L. (2004). From silencing to gene expression: real-time analysis in single cells. Cell *116*, 683–698.

Kaidi, A., Williams, A.C., and Paraskeva, C. (2007). Interaction between β -catenin and HIF-1 promotes cellular adaptation to hypoxia. Nat. Cell Biol. 9, 210–217.

Kelly, K.F., Ng, D.Y., Jayakumaran, G., Wood, G.A., Koide, H., and Doble, B.W. (2011). β -Catenin enhances Oct-4 activity and reinforces pluripotency through a TCF-independent mechanism. Cell Stem Cell 8, 214–227.

Kent, W.J., Sugnet, C.W., Furey, T.S., Roskin, K.M., Pringle, T.H., Zahler, A.M., and Haussler, D. (2002). The human genome browser at UCSC. Genome Res. *12*, 996–1006.

Kouzmenko, A.P., Takeyama, K., Ito, S., Furutani, T., Sawatsubashi, S., Maki, A., Suzuki, E., Kawasaki, Y., Akiyama, T., Tabata, T., and Kato, S. (2004). Wnt/β-catenin and estrogen signaling converge in vivo. J. Biol. Chem. *279*, 40255–40258.

Langmead, B., Trapnell, C., Pop, M., and Salzberg, S.L. (2009). Ultrafast and memory-efficient alignment of short DNA sequences to the human genome. Genome Biol. 10. R25.

Larson, A.G., Elnatan, D., Keenen, M.M., Trnka, M.J., Johnston, J.B., Burlingame, A.L., Agard, D.A., Redding, S., and Narlikar, G.J. (2017). Liquid droplet formation by HP1 α suggests a role for phase separation in heterochromatin. Nature 547, 236–240.

Lee, T.I., and Young, R.A. (2013). Transcriptional regulation and its misregulation in disease. Cell *152*, 1237–1251.

Lin, Y., Protter, D.S.W., Rosen, M.K., and Parker, R. (2015). Formation and Maturation of Phase-Separated Liquid Droplets by RNA-Binding Proteins. Mol. Cell *60*, 208–219.

Lin, C.Y., Erkek, S., Tong, Y., Yin, L., Federation, A.J., Zapatka, M., Haldipur, P., Kawauchi, D., Risch, T., Warnatz, H.-J., et al. (2016). Active medulloblastoma enhancers reveal subgroup-specific cellular origins. Nature 530, 57–62.

Mansour, M.R., Abraham, B.J., Anders, L., Berezovskaya, A., Gutierrez, A., Durbin, A.D., Etchin, J., Lee, L., Sallan, S.E., Silverman, L.B., et al. (2014). An oncogenic super-enhancer formed through somatic mutation of a noncoding intergenic element. Science 346, 1373-1377.

Meyer, K.D., Donner, A.J., Knuesel, M.T., York, A.G., Espinosa, J.M., and Taatjes, D.J. (2008). Cooperative activity of cdk8 and GCN5L within Mediator directs tandem phosphoacetylation of histone H3. EMBO J. 27, 1447-1457.

Molenaar, M., van de Wetering, M., Oosterwegel, M., Peterson-Maduro, J., Godsave, S., Korinek, V., Roose, J., Destrée, O., and Clevers, H. (1996). XTcf-3 transcription factor mediates β-catenin-induced axis formation in Xenopus embryos. Cell 86, 391-399.

Mullen, A.C., and Wrana, J.L. (2017). TGF-β family signaling in embryonic and somatic stem-cell renewal and differentiation. Cold Spring Harb. Perspect.

Mullen, A.C., Orlando, D.A., Newman, J.J., Lovén, J., Kumar, R.M., Bilodeau, S., Reddy, J., Guenther, M.G., DeKoter, R.P., and Young, R.A. (2011). Master transcription factors determine cell-type-specific responses to TGF-β signaling. Cell 147, 565-576.

Nateri, A.S., Spencer-Dene, B., and Behrens, A. (2005). Interaction of phosphorylated c-Jun with TCF4 regulates intestinal cancer development. Nature

Nott, T.J., Petsalaki, E., Farber, P., Jervis, D., Fussner, E., Plochowietz, A., Craggs, T.D., Bazett-Jones, D.P., Pawson, T., Forman-Kay, J.D., and Baldwin, A.J. (2015). Phase transition of a disordered nuage protein generates environmentally responsive membraneless organelles. Mol. Cell 57, 936–947. Nusse, R., and Clevers, H. (2017). Wnt/β-Catenin Signaling, Disease, and

Emerging Therapeutic Modalities. Cell 169, 985-999. Nüsslein-Volhard, C., and Wieschaus, E. (1980). Mutations affecting segment

number and polarity in Drosophila. Nature 287, 795-801. Pak, C.W., Kosno, M., Holehouse, A.S., Padrick, S.B., Mittal, A., Ali, R., Yunus, A.A., Liu, D.R., Pappu, R.V., and Rosen, M.K. (2016). Sequence Determinants

of Intracellular Phase Separation by Complex Coacervation of a Disordered Protein. Mol. Cell 63, 72-85.

Perrimon, N., Pitsouli, C., and Shilo, B.Z. (2012). Signaling mechanisms controlling cell fate and embryonic patterning. Cold Spring Harb. Perspect. Biol. 4, a005975.

Poy, F., Lepourcelet, M., Shivdasani, R.A., and Eck, M.J. (2001). Structure of a human Tcf4-β-catenin complex. Nat. Struct. Biol. 8, 1053–1057.

Rawlings, J.S., Rosler, K.M., and Harrison, D.A. (2004). The JAK/STAT signaling pathway. J. Cell Sci. 117, 1281-1283.

Sabari, B.R., Dall'Agnese, A., Boija, A., Klein, I.A., Coffey, E.L., Shrinivas, K., Abraham, B.J., Hannett, N.M., Zamudio, A.V., Manteiga, J.C., et al. (2018). Coactivator condensation at super-enhancers links phase separation and gene control. Science 361, eaar3958.

Sampietro, J., Dahlberg, C.L., Cho, U.S., Hinds, T.R., Kimelman, D., and Xu, W. (2006). Crystal structure of a β-catenin/BCL9/Tcf4 complex. Mol. Cell 24,

Schindelin, J., Arganda-Carreras, I., Frise, E., Kaynig, V., Longair, M., Pietzsch, T., Preibisch, S., Rueden, C., Saalfeld, S., Schmid, B., et al. (2012). Fiji: an open-source platform for biological-image analysis. Nat. Methods 9, 676-682.

Schuijers, J., Mokry, M., Hatzis, P., Cuppen, E., and Clevers, H. (2014). Wntinduced transcriptional activation is exclusively mediated by TCF/LEF. EMBO J. 33, 146-156.

Shin, Y., and Brangwynne, C.P. (2017). Liquid phase condensation in cell physiology and disease. Science 357, 2415-2423.

Sinner, D., Rankin, S., Lee, M., and Zorn, A.M. (2004). Sox17 and beta-catenin cooperate to regulate the transcription of endodermal genes. Development 131, 3069-3080.

Small, S., Blair, A., and Levine, M. (1992). Regulation of even-skipped stripe 2 in the Drosophila embryo. EMBO J. 11, 4047–4057.

Strom, A.R., Emelyanov, A.V., Mir, M., Fyodorov, D.V., Darzacq, X., and Karpen, G.H. (2017). Phase separation drives heterochromatin domain formation. Nature 547, 241-245.

Takahashi, K., and Yamanaka, S. (2006). Induction of pluripotent stem cells from mouse embryonic and adult fibroblast cultures by defined factors. Cell 126, 663-676.

Takahashi, K., and Yamanaka, S. (2016). A decade of transcription factormediated reprogramming to pluripotency. Nat. Rev. Mol. Cell Biol. 17,

Theunissen, T.W., and Jaenisch, R. (2014). Molecular control of induced pluripotency. Cell Stem Cell 14, 720-734.

Trompouki, E., Bowman, T.V., Lawton, L.N., Fan, Z.P., Wu, D.C., DiBiase, A., Martin, C.S., Cech, J.N., Sessa, A.K., Leblanc, J.L., et al. (2011). Lineage regulators direct BMP and Wnt pathways to cell-specific programs during differentiation and regeneration. Cell 147, 577-589.

van de Wetering, M., Cavallo, R., Dooijes, D., van Beest, M., van Es, J., Loureiro, J., Ypma, A., Hursh, D., Jones, T., Bejsovec, A., et al. (1997). Armadillo coactivates transcription driven by the product of the Drosophila segment polarity gene dTCF. Cell 88, 789-799.

Wang, J., Choi, J.M., Holehouse, A.S., Lee, H.O., Zhang, X., Jahnel, M., Maharana, S., Lemaitre, R., Pozniakovsky, A., Drechsel, D., et al. (2018). A Molecular Grammar Governing the Driving Forces for Phase Separation of Prion-like RNA Binding Proteins. Cell 174, 688-699.e16.

Weintraub, H., Tapscott, S.J., Davis, R.L., Thayer, M.J., Adam, M.A., Lassar, A.B., and Miller, A.D. (1989). Activation of muscle-specific genes in pigment, nerve, fat, liver, and fibroblast cell lines by forced expression of MyoD. Proc. Natl. Acad. Sci. USA 86, 5434-5438.

Whyte, W.A., Orlando, D.A., Hnisz, D., Abraham, B.J., Lin, C.Y., Kagey, M.H., Rahl, P.B., Lee, T.I., and Young, R.A. (2013). Master transcription factors and mediator establish super-enhancers at key cell identity genes. Cell 153, 307-319.

Yan, R., Small, S., Desplan, C., Dearolf, C.R., and Darnell, J.E., Jr. (1996). Identification of a Stat gene that functions in Drosophila development. Cell 84, 421-430.

Yingling, J.M., Datto, M.B., Wong, C., Frederick, J.P., Liberati, N.T., and Wand, X.-F. (1997). Tumor suppressor Smad-4 is a transforming growth factor betainducible DNA binding protein. Mol. Cell. Biol. 17, 7019-7028.

Zhang, Y., Liu, T., Meyer, C.A., Eeckhoute, J., Johnson, D.S., Bernstein, B.E., Nusbaum, C., Myers, R.M., Brown, M., Li, W., and Liu, X.S. (2008). Modelbased analysis of ChIP-Seq (MACS). Genome Biol. 9, R137.

Zhang, X., Choi, P.S., Francis, J.M., Imielinski, M., Watanabe, H., Cherniack, A.D., and Meyerson, M. (2016). Identification of focally amplified lineage-specific super-enhancers in human epithelial cancers. Nat. Genet. 48, 176-182.

Zhang, Y.J., Guo, L., Gonzales, P.K., Gendron, T.F., Wu, Y., Jansen-West, K., O'Raw, A.D., Pickles, S.R., Prudencio, M., Carlomagno, Y., et al. (2019). Heterochromatin anomalies and double-stranded RNA accumulation underlie C9orf72 poly(PR) toxicity. Science 363, eaav2606.

Zhu, F., Farnung, L., Kaasinen, E., Sahu, B., Yin, Y., Wei, B., Dodonova, S.O., Nitta, K.R., Morgunova, E., Taipale, M., et al. (2018). The interaction landscape between transcription factors and the nucleosome. Nature 562, 76-81.

STAR***METHODS**

KEY RESOURCES TABLE

REAGENT or RESOURCE	SOURCE	IDENTIFIER
Antibodies		
GFP	Abcam	ab290; RRID:AB_303395
Med1	Abcam	ab64965; RRID:AB_1142031
β-catenin	Abcam	ab22656; RRID:AB_447227
STAT3	Santa Cruz	SC-7993;RRID:AB_656682
SMAD3	Santa Cruz	SC-6202; RRID:AB_255105
TCF7L2	Santa Cruz	SC-8631; RRID:AB_2199826
TCF1/TCF7	Cell Signaling	2203; RRID:AB_2199302
TCF3/TCF7L1	Cell Signaling	2883; RRID:AB_2199136
LEF1	Cell Signaling	2230; RRID:AB_823558
DsRed	Takara	632496; RRID:AB_0013483
Chemicals, Peptides, and Recombinant Proteins		
mEGFP	This study	N/A
mEGFP-β-catenin	This study	N/A
mEGFP-STAT3	This study	N/A
mEGFP-SMAD3	This study	N/A
mCherry-MED1-IDR	This study	N/A
mEGFP-β-catenin-N terminus	This study	N/A
mEGFP-β-catenin-Armadillo	This study	N/A
mEGFP-β-catenin-C terminus	This study	N/A
mEGFP-β-catenin-Aromatic-Mutant	This study	N/A
mEGFP- β-catenin-chimera	This study	N/A
mEGFP-β-catenin-chimera-mutant	This study	N/A
mEGFP-β-catenin-2XIDR	This study	N/A
Full Mediator	This study	N/A
CHIR99021	Stemgent	04-0004
Leukemia Inhibitory Factor (LIF)	ESGRO	ESG1107
Activin A	R&D systems	338-AC-010
IWP2	Sigma Aldrich	10536
SB431542	Tocris Bioscience	16-141
Critical Commercial Assays		
Dual-glo Luciferase Assay System	Promega	E2920
NEBuilder HiFi DNA Assembly Master Mix	NEB	E2621S
Power SYBR Green mix	Life Technologies	4367659
TaqMan Universal PCR Master Mix	Applied Biosystems	4304437
RNeasy Plus Mini Kit	QIAGEN	74136
Sp5 probe	Taqman	Mm00491634_m1
Myc probe	Taqman	Mm00487804_m1
Gapdh probe	Taqman	Mm9999915_g1
Deposited Data	· · · · · · · · · · · · · · · · · · ·	
Med1 ChIP-seq	This study	GenBank: GSE134387
GFP-β-catenin ChIP-seq	This study	GenBank: GSE134387
GFP-armadillo ChIP-seq	This study	GenBank: GSE134387
GFP-chimera ChIP-seq	This study	GenBank: GSE134387
		(Continued on next page

(Continued on next page)

REAGENT or RESOURCE	SOURCE	IDENTIFIER
Imaging data	This study	https://doi.org/10.17632/x4j73x87bj.1
Imaging data	This study This study	https://doi.org/10.17632/99bt56v4zs.1
,	This study	11ttps://doi.org/10.17002/9901000425.1
Experimental Models: Cell Lines	D 1 K 1	NIA
V6.5 cells	Rudolf Jaenisch	N/A
β-catenin-GFP-tagged V6.5 cells	This study	N/A
β-catenin-GFP-tagged HCT116 cells	This study	N/A
Hp1α-GFP-tagged HCT116 cells	This study	N/A
C2C12 cells	ATCC	N/A
HEK293T cells	ATCC	N/A
TdTomato-wild-type-β-catenin V6.5 cells	This study	N/A
TdTomato-aromatic-mutant-β-catenin V6.5 cells	This study	N/A
U2OS-2-6-3 cells	Spektor Lab	N/A
GFP-chimera HEK293T cells	This study	N/A
GFP-chimera-mutant HEK293T cells	This study	N/A
GFP-armadillo V6.5 cells	This study	N/A
GFP-chimera V6.5 cells	This study	N/A
Oligonucleotides		
Oligonucleotides used in this study are listed in Table S1	This study	N/A
Recombinant DNA	·	
pJM101-PiggyBac-BetaCat-FL	This study	N/A
pJM102-PiggyBac-BetaCat-AromaticMut	This study	N/A
pJS-21-mEGFP-Bcat-repair-mo	This study	N/A
pJS-22-mEGFP-Bcat-repair-hu	This study	N/A
pX330-GFP-B-catenin	This study	N/A
Software and Algorithms		
Fiji image processing package	Schindelin et al., 2012	https://fiji.sc/
MetaMorph acquisition software	Molecular Devices	https://www.moleculardevices.com/products cellular-imaging-systems/acquisition-and- analysis-software/metamorph-microscopy
PONDR	http://www.pondr.com/	N/A
MACS	Zhang et al., 2008	N/A
Bowtie	Langmead et al., 2009	N/A
Other		
Nanog RNA FISH probe	Stellaris	N/A
miR290 RNA FISH probe	Stellaris	N/A
Nanog DNA FISH probe	Agilent	N/A

LEAD CONTACT AND MATERIALS AVAILABILITY

Further information and requests for resources and reagents should be directed to and will be fulfilled by the Lead Contact, Richard A. Young (young@wi.mit.edu).

EXPERIMENTAL MODEL AND SUBJECT DETAILS

Cell lines

V6.5 murine embryonic stem cells were a gift from the Jaenisch lab. HEK293T and HCT116 cells were obtained from ATCC. U2OS cells were obtained from the Spector lab. Cells were routinely tested for mycoplasm.

Cell culture conditions

V6.5 murine embryonic stem cells were grown on 2i + LIF conditions on 0.2% gelatinized (Sigma, G1890) tissue culture plates. The media used for 2i + LIF media conditions is as follows: 967.5 mL DMEM/F12 (GIBCO 11320), 5 mL N2 supplement (GIBCO 17502048), 10 mL B27 supplement (GIBCO 17504044), 0.5 mM L-glutamine (GIBCO 25030), 0.5X non-essential amino acids (GIBCO 11140), 100 U/mL Penicillin-Streptomycin (GIBCO 15140), 0.1 mM β-mercaptoethanol (Sigma), 1 uM PD0325901 (Stemgent 04-0006), 3 uM CHIR99021 (Stemgent 04-0004), and 1000 U/mL recombinant LIF (ESGRO ESG1107). HEK293T, U2OS and HCT116 cells were cultured in DMEM, high glucose, pyruvate (GIBCO 11995-073) with 10% fetal bovine serum (Hyclone, characterized SH3007103), 100 U/mL Penicillin-Streptomycin (GIBCO 15140), 2 mM L-glutamine (Invitrogen, 25030-081). Sf9 cells were cultured in Sf-900 III SFM (GIBCO 12658-019) supplemented with 0.017mg/ml of penecilin streptomycin (GIBCO 15140).

Cell line stimulation

For WNT: Cells were treated with either CHIR99021 or IWP2 (Sigma Aldrich I0536) for 24hrs in 2i + LIF medium without CHIR (mES) or with CHIR in 10% FBS DMEM medium (HEK293).

For SMAD3: Cells were treated with ActivinA (R&D systems 338-AC-010) or SB431542 (Tocis Bioscience 16-141) for 24 hours in 2i + LIF medium. For STAT3: Cells were treated with 2i + LIF or 2i - LIF medium for 24 hours

Cell line generation

V6.5 murine embryonic stem cells, HCT116 colorectal cancer cells or HEK293T embryonic kidney cells were genetically modified using the CRISPR-Cas9 system. A guide targeting the N terminus of beta catenin was cloned into a px330 vector with an mCherry selectable marker and the following sequence: CTGCGTGGACAATGGCTACT. A repair template with 800 bp homology to the endogenous locus flanking an mEGFP-tag was cloned into a pUC19 vector. Cells were transfected with 2.5 μ g of both constructs and sorted for mCherry two days post-transfection and sorted again for mEGFP one week post-transfection. Cells were serially diluted and colonies were picked to obtain clonal cell lines.

METHOD DETAILS

FRAP

FRAP was performed on LSM880 Airyscan microscope with 488nm laser. Bleaching was performed over a $r_{bleach} \approx 1$ um using 100% laser power and images were collected every two seconds.

Immunofluorescence

Cells were fixed in 4% paraformaldehyde for 10 mins at RT as described in Sabari et al. (2018). Cells were then washed three times and permeabilized with 0.5 Triton X-100 in PBS for 5 min at RT. Following three washes in PBS cells were blocked in 4% Bovine Serum Albumin for 15 mins at RT and incubated with primary antibodies in 4% BSA overnight at room temperature. After three washes in PBS, cells were incubated in secondary antibodies in 4% BSA in the dark for 1 hour. Cells were washed three times with PBS followed by an incubation with Hoechst for 5 mins at RT in the dark. Slides were mounted with Vectashield H-1000 and coverslips were sealed with transparent nail polish and stored at 4°C. Images were acquired using an RPI Spinning Disk confocal microscope with a 100x objective using a Metamorph software and a CCD camera.

Co-Immunofluorescence with DNA FISH

Immunofluorescence was performed as described earlier with modifications to the protocol following incubation with secondary antibodies. After secondary antibodies cells were washed 3 times in PBS at RT and then fixed with 4% PFA in PBS for 20 mins and washed three times with PBS. Cells were incubated in 70% ethanol, 85% ethanol and then 100% ethanol for 1 min at RT. Probe hybridization mixture was made with 7μl of FISH Hybridization Buffer (Agilent G9400A), 1 μl of FISH probes and 2μl of water. 5μl of mixture was added on a slide and coverslip was placed on top. Coverslip was sealed using rubber cement. Once rubber cement solidified genomic DNA and probes were denatured at 78°C for 5 mins and slides were incubated at 16°C in the dark overnight. Coverslips were removed from the slide and incubated in a pre-warmed Wash Buffer 1 at 73°C for 3 mins and in Wash Buffer 2 for 1 min at RT. Slides were air-dried and nuclei stained with Hoechst in PBS for 5 mins at RT. Coverslips were washed three times in PBS, mounted on a slide using Vectashield H-1000 and sealed with nail polish. Images were acquired using an RPI Spinning DIsk confocal microscope with a 100x objective using the MetaMorph acquisition software and a Hammamatsu ORCA-ER CCD Camera. DNA FISH probes were custom designed and generated by Agilent to target the Nanog locus.

Co-Immunofluorescence with RNA FISH

Immunofluorescence was performed as previously described (Sabari et al., 2018) with the small modifications. Immunofluorescence was performed in a RNase-free environment, pipettes and bench were treated with RNaseZap (Life Technologies, AM9780). RNase free PBS was used and antibodies were diluted in RNase-free PBS at all times. After immunofluorescence completion. Cells were post-fixed with 4% PFA in PBS for 10 min at RT. Cells were washed twice with RNase-free PBS. Cells were washed once with 20% Stellaris RNA FISH Wash Buffer A (Biosearch Technologies, Inc., SMF-WA1-60), 10% Deionized Formamide (EMD Millipore,

S4117) in RNase-free water (Life Technologies, AM9932) for 5 min at RT. Cells were hybridized with 90% Stellaris RNA FISH Hybridization Buffer (Biosearch Technologies, SMF-HB1-10), 10% Deionized Formamide, 12.5 µM Stellaris RNA FISH probes designed to hybridize introns of the transcripts of SE-associated genes. Hybridization was performed overnight at 37°C. Cells were then washed with Wash Buffer A for 30 min at 37°C and nuclei were stained with 20μm/ml HOESCHT in Wash Buffer A for 5 min at RT. After one 5-min was with Stellaris RNA FISH Wash Buffer B (Biosearch Technologies, SMF-WB1-20) at room temperature. Coverslips were mounted as described for immunofluorescence. Images were acquired at the RPI Spinning Disk confocal microscope with 100x objective using MetaMorph acquisition software and a Hammamatsu ORCA-ER CCD camera. Primary antibodies used were anti-MED1 Abcam ab64965 1:500 dilution, anti-b catenin Abcam ab22656 1:500 dilution, anti-pSTAT3 Santa Cruz 1:20 dilution, anti-SMAD2/3 Santa Cruz 1:20 dilution). Secondary antibodies used were anti-Rabbit IgG, anti-goat IgG and anti-mouse IgG.

Protein purification

cDNA encoding the genes of interest or their IDRs were cloned into a modified version of a T7 pET expression vector. The base vector was engineered to include a 5' 6xHIS followed by either mEGFP or mCherry and a 14 amino acid linker sequence "GAPGSAG SAAGGSG." NEBuilder® HiFi DNA Assembly Master Mix (NEB E2621S) was used to insert these sequences (generated by PCR) in-frame with the linker amino acids. Vectors expressing mEGFP or mCherry alone contain the linker sequence followed by a STOP codon. Mutant sequences were synthesized as geneblocks (IDT) and inserted into the same base vector as described above. All expression constructs were sequenced to ensure sequence identity.

For protein expression plasmids were transformed into LOBSTR cells (gift of Chessman Lab) and grown as follows. A fresh bacterial colony was inoculated into LB media containing kanamycin and chloramphenicol and grown overnight at 37°C. Cells containing the MED1-IDR constructs were diluted 1:30 in 500ml room temperature LB with freshly added kanamycin and chloramphenicol and grown 1.5 hours at 16°C. IPTG was added to 1mM and growth continued for 18 hours. Cells were collected and stored frozen at -80°C. Cells containing all other constructs were treated in a similar manner except they were grown for 5 hours at 37°C after IPTG induction. The 2X IDR β-catenin protein was expressed in Baculovirus infected Sf9 cells. Bacmid transfections were performed using Cellfectin II reagent (Thermo 10362100) per manufacturer recommendations.

Pellets of 500ml of Beta Catenin mutant cells were resuspended in 15ml of denaturing buffer (50mM Tris 7.5, 300mM NaCl, 10mM imidazole, 8M Urea) containing cOmplete protease inhibitors (Roche, 11873580001) and sonicated (ten cycles of 15 s on, 60 s off). The lysates were cleared by centrifugation at 12,000 g for 30 minutes and added to 1ml of pre-equilibrated Ni-NTA agarose (Invitrogen, R901-15). Tubes containing this agarose lysate slurry were rotated for 1.5 hours at room temperature. The slurry was centrifuged at 3,000 rpm for 10 minutes in a Thermo Legend XTR swinging bucket rotor. The pellets were washed 2 X with 5ml of lysis buffer followed by centrifugation 10 minutes at 3,000 rpm as above. Protein was eluted 3 X with 2ml of the lysis buffer with 250mM imidazole. For each cycle the elution buffer was added and rotated at least 10 minutes and centrifuged as above. Eluates were analyzed on a 12% acrylamide gel stained with Coomassie. Fractions containing protein of the expected size were pooled, diluted 1:1 with the 250mM imidazole buffer and dialyzed first against buffer containing 50mM Tris pH 7.5, 125Mm NaCl, 1mM DTT and 4M Urea, followed by the same buffer containing 2M Urea and lastly 2 changes of buffer with 10% Glycerol, no Urea. Any precipitate after dialysis was removed by centrifugation at 3.000rpm for 10 minutes. MED1-IDR, WT Beta Catenin and 2X IDR Beta Catenin were purified in a similar manner except the lysis buffer contained no urea, the incubations were done at 4C and dialysis was into 2 changes of 50mM Tris pH7.5, 125mM NaCl, 10% glycerol and 1mM DTT.

In vitro droplet formation assay

Recombinant GFP or mCherry fusion proteins were concentrated and desalted to an appropriate protein concentration and 125mM NaCl using Amicon Ultra centrifugal filters (30K MWCO, Millipore). Recombinant proteins were added to solutions at varying concentrations with indicated final salt and 10% PEG-8000 as crowding agent in Droplet Formation Buffer (50mM Tris-HCl pH 7.5, 10% glycerol, 1mM DTT). The protein solution was immediately loaded onto a homemade chamber comprising a glass slide with a coverslip attached by two parallel strips of double-sided tape. Slides were then imaged with an Andor confocal microscope with a 150x magnification. Unless indicated, images presented are of droplets settled on the glass coverslip.

Coverslips were coated with PEG-silane in order to neutralize charge. In brief, coverslips were washed with 2% Helmanex III for 2 hours, washed with H₂O three times and washed with ethanol once before being incubated in 0.5% PEG-silane in ethanol with 1% Acetic Acid over night. They were then washed with ethanol once and sonicated in a water bath sonicator for 15 minutes in ethanol, washed with H₂O for three times before being rinsed with ethanol and dried to the air.

Droplet Assays in Nuclear Extract

Coding sequence of desired genes were cloned into a mammalian expression vector (modified from Addgene #32104) containing either mEGFP or mCherry. These vectors were transfected into 20×10^6 HEK293T cells using PEI transfection reagent (Polysciences Catalog# 23966). 48 hr post transfection, cells were resuspended in 10 mL HMSD50 buffer (20mM HEPES, 5mM MgCl2 250mM sucrose, 1mM DTT, 50mM NaCl supplemented with 0.2 mM PMSF and 5 mM sodium butyrate) and incubated for 30 min at 4°C with gentle agitation. The solution was spun down at 3500 rpm at 4°C for 10 min. The supernatant was discarded and the pellet containing nuclei were washed in Mnase buffer (20mM HEPES, 100mM NaCl, 5mM MgCl2, 5mM CaCl2, protease and phosphatase inhibitors). The washed nuclei were resuspended in one pellet volume of Mnase buffer and treated with 1u Mnase (Sigma #N3755) at 37°C for

10 min. One pellet volume of stop buffer (20mM HEPES, 500mM NaCl, 5mM MgCl2, 30% glycerol, 15mM EGTA, protease and phosphatase inhibitors) was added to stop the reaction. The solution was briefly sonicated and spun down at 3500 rpm at 4°C for 10 min. The supernatant was spun down again at 3500 rpm at 4°C for 5 min to clear the nuclear extract. The nuclear extract (\sim 10 mg/ml) was used for droplet formation assays. The concentrations of the overexpressed proteins within nuclear extracts were measured by dot blot using recombinant mEGFP or mcherry as standard: mEGFP or GFP tagged B-catenin: 5 μ M; mEGFP: 25 μ M; mcherry: 40 μ M; MECP2: 20 μ M; MED12: 5 μ M. Droplet formation was induced by 1:1 dilution of the nuclear extract with Buffer B (10% glycerol, 20mM HEPES). The final droplet buffer conditions were 20mM HEPES, 150mM NaCl, 15% glycerol, 3.75mM EGTA, 2.5mM MgCl2, 1.25mM CaCl2. The reactions were incubated for 30 min in 8-well PCR strips and loaded onto glass bottom 384 well plate (Cellvis P384-1.5H-N) 5 min prior to imaging on an Andor confocal microscope at 150X magnification.

Purification of Mediator

Mediator samples were purified as previously described (Meyer et al., 2008, https://doi.org/10.1038/emboj.2008.78) with modifications. The P0.5M/QFT fraction was concentrated, to 12 mg/mL, by ammonium sulfate precipitation (35%). The resulting pellet was resuspended in pH 7.9 buffer containing 20 mM KCl, 20 mM HEPES, 0.1 mM EDTA, 2 mM MgCl2, 20% glycerol and dialyzed against pH 7.9 buffer containing 0.15 M KCl, 20 mM HEPES, 0.1 mM EDTA, 20% glycerol, and 0.02% NP-40 prior to the affinity purification step. Affinity purification was carried out as described (Meyer et al., 2008, https://doi.org/10.1038/emboj.2008.78).

RT-qPCR

RNA was isolated using the Rneasy Plus Mini Kit (QIAGEN, 74136) according to manufacturer's instructions. cDNA was generated using SuperScript II Reverse Transcriptase (Invitrogen, 18080093) with oligo-dT primers (Promega, C1101) according to manufacturer's instructions. Quantitative real-time PCR was performed on Applied Biosystems 7000, QuantStudio5 and QuantStudio6 instruments using TaqMan probes for SE genes.

ChIP

Cells were plated at a density of 4-5 million cells per plate and harvested 24-48 hours after. 1% formaldehyde in PBS was used for crosslinking of cells for 15 minutes, followed by guenching with Glycine at a final concentration of 125mM on ice. Cells were washed with cold PBS and harvested by scraping cells in cold PBS. Collected cells were pelleted at 1500 g for 5 minutes at 4°C, resuspended in LB1 (50mM HEPES- KOH, pH7.9, 140mM NaCl, 1mM EDTA 0.5mL 0.5M, 10% glycerol, 0.5% NP40, 1% Triton X-100, 1x protease inhibitor) and incubate for 20 minutes rotating at 4°C. Cells were pelleted for 5 minutes at 1350 g, resuspended in LB2 (10 mM Tris pH 8.0, 200 mM NaCl, 1 mM EDTA, 0.5 mM EGTA, 1x protease inhibitor) and incubated for 5 minutes rotating at 4°C. Pellet was resuspended in LB3 (10 mM Tris pH 8.0, 100 mM NaCl, 1 mM EDTA, 0.5 mM EGTA, 0.1% sodium-deoxycholate, 0.5% sodium lauroyl sarcosinate, 1% Triton X-100, 1x protease inhibitor) at a concentration of 30-50 million cells/ml. Cells were sonicated using Covaris S220 for 12 minutes using the manufacturer's instructions followed by spinning at 20 000 g for 30 minutes at 4°C. Dynabeads preblocked with 0.5% BSA were incubated with GFP antibody (Abcam, ab290), Med1 antibody (Abcam, ab64965) or dsRed (Takara, 632496) antibody for 6 hours. Chromatin was added to antibody-bead complex and incubated rotating overnight at 4°C. Beads were washed three times with each Wash buffer 1 (50mM HEPES pH7.5, 500mM NaCl, 1mM EDTA, 1mM EGTA,1% Triton, 0.1% NaDoc, 0.1% SDS) and Wash Buffer 2 (20mM Tris pH 8, 1mM EDTA, 250mM LiCl, 0.5% NP40, 0.5% NaDoc) at 4°C, followed by washing one time with TE at room temperature. Chromatin was eluted by adding Elution buffer (50 mM, Tris pH 8.0, 10 mM EDTA, 1% sodium dodecyl sulfate, 20ug/ml RNaseA) to the beads and incubated shaking at 60°C for 30 minutes. Reversal of crosslinking was performed for 4 hours at 58°C. Proteinase K was added and incubated for 1-2 hours at 37°C for protein removal. DNA was purified using QIAGEN PCR purification kit and resuspended in 10mM Tris-HCL. ChIP Libraries were prepared with the Swift Biosciences Accel-NGS® 2S Plus DNA Library Kit according to kit instructions with an additional size selection step on the PippinHT system from Sage Science. Following library prep, ChIP libraries were run on a 2% gel on the PippinHT with a size collection window of 200-600 bases. Final libraries were quantified by qPCR with the KAPA Library Quantification kit from Roche and sequenced in singleread mode for 40 bases on an Illumina HiSeq 2500.

QUANTIFICATION AND STATISTICAL ANALYSIS

FRAP quantification

Fluorescence intensity was measured using FIJI. Background intensity was subtracted and values are reported relative to prebleaching time points.

Custom MATLAB scripts were written to process the intensity data, accounting for background photobleaching and normalization to pre-bleach intensity. Post bleach FRAP recovery data was averaged over 9 replicates for each cell-line and condition. The FRAP recovery curve was fit to:

$$FRAP(t) = M\left(1 - \exp\left(-\frac{t}{\tau}\right)\right)$$

Average image analysis

For analysis of RNA FISH with immunofluorescence, custom MATLAB scripts were written to process and analyze 3D image data gathered in RNA FISH and IF channels. FISH foci

were identified in individual z stacks through intensity and size thresholds, centered along a box of size $l = 2.9 \mu m$ and stitched together in 3-D across z stacks. For every FISH focus identified, signal from the corresponding location in the IF channel is gathered in the I x I square centered at the RNA FISH focus at every corresponding z-slice. The IF signal centered at FISH foci for each FISH and IF pair are then combined and an average intensity projection is calculated, providing averaged data for IF signal intensity within a I x I square centered at FISH foci. The same process was carried out for the FISH signal intensity centered on its own coordinates, providing averaged data for FISH signal intensity within a l; x l; square centered at FISH foci. As a control, this same process was carried out for IF signal centered at randomly selected nuclear positions. For each replicate, 40 random nuclear points were generated from the interior of the nuclear envelope, identified from the DAPI channel by a combination of large size (200 voxels) and intensity (DNA dense) thresholds. These average intensity projections were then used to generate 2D contour maps of the signal intensity. Contour plots are generated using built-in functions in MATLAB. For the contour plots, the intensity-color ranges presented were customized across a linear range of colors (n! = 15). For the FISH channel, black to magenta was used. For the IF channel, we used chroma.js (an online color generator) to generate colors across 15 bins, with the key transition colors chosen as black, blueviolet, mediumblue, lime. This was done to ensure that the reader's eye could more readily detect the contrast in signal. The generated colormap was employed to 15 evenly spaced intensity bins for all IF plots. The averaged IF centered at FISH or at randomly selected nuclear locations are plotted using the same color scale, set to include the minimum and maximum signal from each plot.

Heterotypic droplet analysis

To analyze in vitro droplet experiments, custom Python scripts using the scikit-image package were written to identify droplets and characterize their size, shape, and intensity. Droplets were segmented from average images of captured channels on various criteria: (1) an intensity threshold three standard deviations above the mean of the image, (2) size thresholds (9 pixel minimum droplet size), (3)

and a minimum circularity
$$\left(\text{circularity} = 4\pi * \frac{\text{area}}{\text{perimiter}^2} \right)$$
 of 0.8 (1 being a perfect circle). After segmentation, mean intensity for each

droplet was calculated while excluding pixels near the phase interface (Banani et al., 2017). Hundreds of droplets identified in typically 5-10 independent fields of view were quantified. The mean intensity within the droplets (C-in) and in the bulk (C-out) were calculated for each channel. The partition ratio was computed as (C-in)/(C-out). The boxplots show the distributions of all droplets. The measured datasets for partition ratio versus the protein concentration in Figure 2B were fitted by the logistic equation (Wang et al., 2018):

$$f = \frac{a}{1 + e^{-\frac{(x - x0)}{b}}}$$

Where *f* is the partition ratio and *x* is the corresponding protein concentration.

ChIP-seg analysis

ChIP-Seq data were aligned to the mm9 version of the mouse reference genome using bowtie with parameters -k 1 -m 1 -best and -l set to read length. Wiggle files for display of read coverage in bins were created using MACS with parameters -w -S space = 50 -nomodel -shiftsize = 200, and read counts per bin were normalized to the millions of mapped reads used to make the wiggle file (Zhang et al., 2008). Reads-per-million normalized wiggle files were displayed in the UCSC genome browser (Kent et al., 2002)

DATA AND CODE AVAILABILITY

All software and code generated in this project are publicly available at: https://github.com/jehenninger/FISH_IF and https://github. com/jehenninger/in_vitro_droplet_assay

ChIP-seq data were deposited into GEO under the accession number GEO: GSE134387.

Raw images associated with presented figures have been deposited in the Mendeley databases: https://doi.org/10.17632/ x4j73x87bj.1 https://doi.org/10.17632/99bt56v4zs.1